

Molecular Screening of Amino Acid Ionic Liquids in CO₂ Capture via COSMO-RS and DFT

Jivana Parameswaran^{1,2}, Noraini Abd Ghani^{1,2*}, Khairulazhar Jumbri^{1,2} and Normawati Bt. M. Yunus^{1,2}

¹Center of Research in Ionic Liquids (CORIL), Universiti Teknologi PETRONAS, 32610 Seri Iskandar, Perak, Malaysia

²Department of Fundamental and Applied Sciences, Universiti Teknologi PETRONAS, 32610 Seri Iskandar, Perak, Malaysia

*Corresponding author (noraini.ghani@utp.edu.my)

Ionic liquids (ILs) are one of the main focuses of researchers to replace conventional solvents as they are known as 'green' solvents and possess many advantages. Recently, direct air capture (DAC) of carbon dioxide (CO₂) systems has become the subject of extensive scientific study, as it causes severe effects on the environment and humans. Carbon capture is one of the techniques that could be used to reduce CO₂ emissions. This study used a conductor-like screening model for real solvents (COSMO-RS) as an initial screening tool to design and identify the performance between anions and cations of amino acid ILs (AAILs) for CO₂ capture. The chosen best-performance AAILs are Tetrabutylammonium and Tetrabutylphosphonium paired with phenylalanine, serine, glycine, and aspartate. The results were compared with the density functional theory (DFT) calculation and molecular modelling. Moreover, the viscosity and ionic conductivity of the chosen AAILs were also studied. The significance of this study is to reduce time and expenses in selecting acceptable AAILs and comparing their CO₂ capture performance via COSMO-RS and DFT. It should also boost the chances of finding new task-specific ILs (TSILs).

Keywords: CO₂ capture; ionic liquid; amino acid ionic liquids; task-specific ionic liquids; COSMO-RS; DFT

Received: March 2024; Accepted: June 2024

A variety of gases make up the Earth's atmosphere: oxygen, argon, water vapour, and CO₂ [1]. Even though the percentage of CO₂ in ambient air is only 0.04%, it has a greater molar mass (MM) and density than other gases. The MM of CO₂ is 44 g/mol, which is approximately 30% higher than other air compositions. CO₂ will gather in low regions for short periods under calm conditions, but it will evaporate in a few hours, or days at most. Large CO₂ emissions can be harmful, although it is short-lived. Table 1 shows the compound, percentage, MM, and density (ρ) of each of the gases present in the air.

In today's world, the temperature of the Earth is steadily rising, which is quite risky and disturbing

[2]. Coal, natural gas, and crude oil keep on being the key worldwide energy sources. Consequently, large amounts of CO₂ are emitted into the atmosphere, causing the Earth's surface temperature to rise significantly [2-6]. According to the Intergovernmental Panel on Climate Change (IPCC), mainly due to manmade CO₂ emissions, the atmospheric concentration of CO₂ has dramatically grown from around 280 ppm to more than 412 ppm [6]. Excessive CO₂ emissions contribute significantly to global warming [4,6,7], resulting in negative climate change, glacier melting [4,5], ecological environment degradation [6,7,], and spread of deadly illnesses (e.g., cholera, malaria, COVID-19) [6].

Table 1. Composition of ambient air [1].

Compound	Composition percentage (%)	Molar mass (g/mol)	Density (kg/m ³)
N ₂	78.1%	28.0	1.25
O ₂	20.9%	32.0	1.43
Ar	0.9%	39.96	1.69
CO ₂	0.04%	44.00	1.87

CO₂ may be dissolved in conventional ILs (such as, imidazolium-based ILs), which offers the opportunity to build innovative CO₂ capture systems [8]. However, these approaches have several disadvantages, including pollution, inefficiency, expensive costs [8], and toxicity. Commercial ILs are also known as 'greener' solvents which can capture CO₂ under atmospheric conditions but the solubility of CO₂ in conventional ILs is limited. In TSILs, the functional group is covalently attached to the cation or anion (or both) which can be targeted to a specific application. This capability allows the ILs to function not only as a reaction medium but also as a catalyst in some reactions. TSILs are effective alternatives for volatile organic compounds (VOCs) in organic synthesis. TSILs are used as catalysts or solvents in organic processes, where they offer a less harmful reaction medium than typical organic solvents and the ability to be recycled without losing their high catalytic activity. This is one of the most reported applications of TSILs. To increase the activity and catalytic selectivity in various chemical synthesis, several TSILs have also been applied as solid catalyst surface modifiers. In this context, it is valuable to note the abundant literature that focuses on how TSILs are used in CO₂ chemistry. CO₂ is currently a subject of great interest as it is considered the most significant greenhouse gas. TSILs have been employed as green chemisorb, catalysts, or promoters for absorption, capture, and subsequent conversion because of their minimal volatility [9].

TSILs are commonly categorised into three groups based on the locations of their active sites: cation-functionalised ILs, anion-functionalised ILs, and cation-anion dual-functionalised ILs. AAILs fall under the category of anion-functionalised ILs [9]. AAILs have better absorption capacity and considerable synthesis cost. AAILs contain amino groups (-NH₂) like amines, which play a role in reacting with CO₂ and enhancing CO₂ absorption [10,11]. Therefore, AAILs are significantly used to capture CO₂ as they have many advantages. AAs have a unique position among biomolecules in that they may be readily transformed into both anions and cations, and the diversity of functional groups found in their side chains allows for the easy insertion of chirality and a broad range of functionalities into the ILs. In comparison to the rest of the chiral pool, AAs are inexpensive and abundant. Therefore, AAILs play an important role in green and sustainable chemistry [12].

It might be difficult to choose possible ILs from a variety of anion-cation combinations. COSMO-RS has become an effective method for screening solvents based on a range of fluid combination parameters to resolve this problem [13]. Additionally, a distinct method is used to technically describe how the AAILs, and solutes (CO₂), behave in molecular modelling. The solubility of CO₂ from the optimised

shape may be explained via hydrogen bond interaction [14].

In this study, COSMO-RS was used in screening 440 AAILs, which would be employed for CO₂ capture application from combinations of 22 cations and 20 AA anions. This project aims to design AAILs with a greater ability for CO₂ capture in a systemic way by using COSMO-RS as an initial screening tool and the best-performance AAILs will be chosen to undergo molecular modelling to confirm the results. It is also capable of reducing time and expense in selecting acceptable AAILs.

METHODOLOGY

Structure Optimisation

The geometrical structures of cations and anions were optimised separately using DFT implemented by applying Becke and Perdew (BP) functional with triple zeta valence polarised (TZVP) [15]. Therefore, the basic set B3-LYP/ def2_TZVPD level was used, and the files were generated using the TURBOMOLE software (Tmolex) version 18.

COSMO-RS is used for predicting thermophysical parameters in a wide range of systems. In COSMO-RS calculations, ILs are considered equimolar combinations of cations and anions [15], and the results are considered for the pure ILs. The optimised structures in Tmolex were saved as (.cosmo) for the study in COSMO-RS.

Then, for the molecular modelling, the structures of ILs-CO₂ were optimised using the same basic set to study the interaction and the files were saved as (.pse) in Tmolex to be used in the Pymol software.

Property calculation of COSMO-RS

Table 2 shows the properties that need to be studied in COSMO-RS and Figure 1 shows the procedure to design AAILs with various anions and cations, as well as to determine the CO₂ capture capacity of the designed AAILs using the COSMO-RS software. Equation 1 enables the calculation of selectivity, while Equation 2 is employed to determine capacity, and Equation 3 is utilised to assess the performance index of AAILs, as detailed in Table 2. The simulation will be conducted with 1 atm pressure and 25°C (298.15 K) [15] in COSMOterms version 19 software with parameterisation of TZVPD-Fine.

The AAILs demonstrating the most effective performance in CO₂ capture will be selected for further investigation of viscosity and ionic conductivity at various temperatures using the COSMO-RS approach. This analysis will be closely linked to the overall performance of the AAILs.

Table 2. Properties that need to be studied in COSMO-RS.

PROPERTIES	DEFINITION
Sigma Surface	3D representation of charge polarisation just on the surface of molecules [16].
Sigma Profile	Reflects the polarity of the tested compound [16].
Sigma Potential	Estimated as the total sigma profile of all the components [17]. Identifies the hydrophobic or hydrophilic characteristic.
Activity coefficient	Related to the solubilising power of ILs [17].
Henry Constant	Related to gas solubility [13].
Solvation Energy	The amount of energy needed to dissolve a solute in a solvent [13].
Selectivity	Related to gas solubility/ interaction potential of ILs with 2 specific gases [18]. $S_{(CO_2/N_2)}^{\infty} = (\gamma_{CO_2}^{\infty} / \gamma_{N_2 \text{ or } O_2}^{\infty})^{IL}$ (Equation 1)
Capacity	Absorption capability of gas [15]. $C^{\infty} = (1/\gamma_1^{\infty})^{IL}$ (Equation 2)
Performance Index	Assesses the performance and efficacy of any solvent in accomplishing the absorption [15]. $PI = S_{(CO_2/N_2 \text{ or } O_2)}^{\infty} \times C_{(CO_2)}^{\infty}$ (Equation 3)

Flow of COSMO-RS

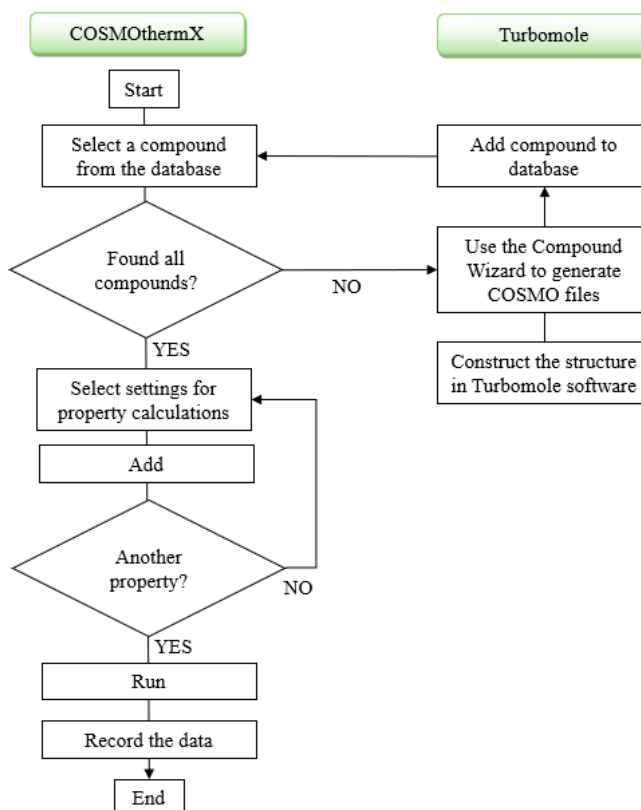


Figure 1. Flow chart of the property calculation with COSMO-RS software.

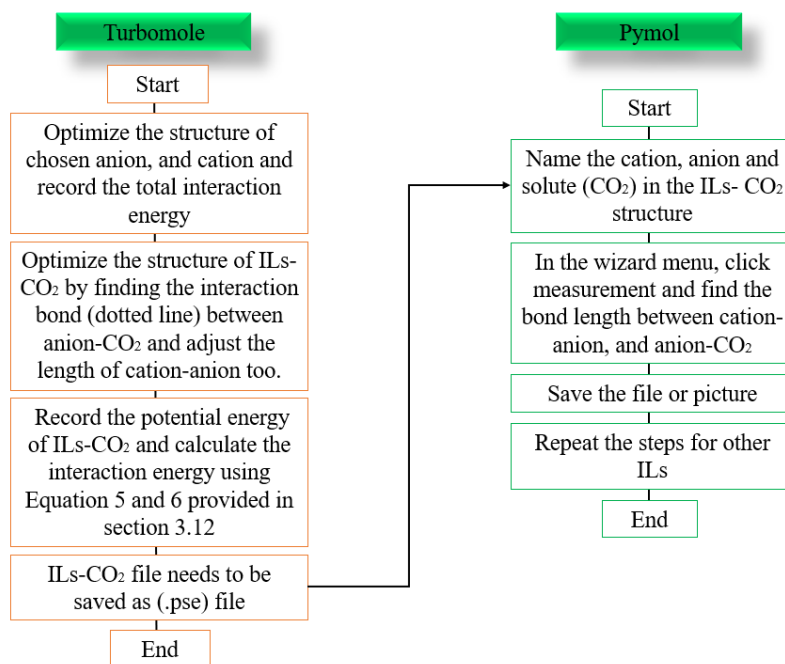


Figure 2. Flow chart of DFT.

Flow Chart of Density Functional Theory and Molecular Modelling

The best-performance AAILs from the COSMO-RS were chosen to study the interaction energy of anions, cations, and ILs-CO₂ using the Tmolex software (DFT calculation) and bond length using the Pymol software (molecular modelling). Figure 2 shows the procedure to study the interaction energy and bond length of ILs-CO₂.

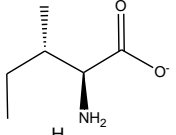
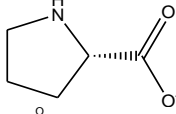
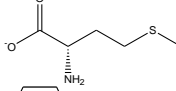
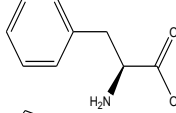
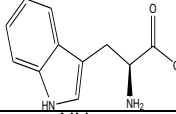
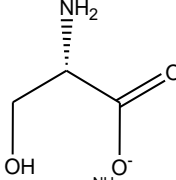
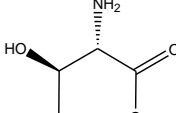
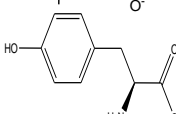
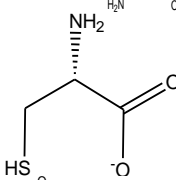
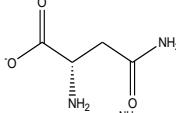
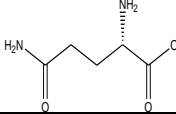
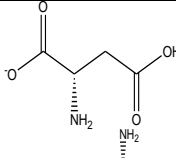
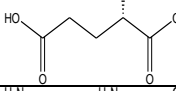
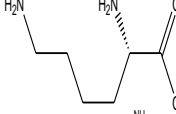
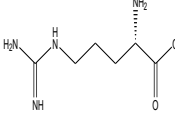
Designation of AAILs

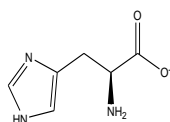
Based on the associations above, we proposed a few amine candidates as prospective CO₂ capture

possibilities. The Practical Handbook of Biochemistry and Molecular Biology contains a comprehensive list of over 300 AAs. However, Table 3 highlights only the 20 AAs utilised to create AAILs in this project. The type of the R substituent is the main difference between most of the AAs. The common AAs are therefore categorised based on these R groups. AAs having non-polar substituents are said to be hydrophobic (water-hating). On the other hand, AAs with polar substituents are hydrophilic (water-loving). The other AAs contain substituents that carry either negative or positive charges in an aqueous solution at neutral pH and are consequently highly hydrophilic [19].

Table 3. Twenty common anions used for AAIL design in this study.

ANIONS			
Structure	Name	Abbr.	MM (g/mol)
	Glycinate	GLY	74.02
	Alaninate	ALA	88.09
	Valinate	VAL	116.14
	Leucinate	LEU	130.17

	Isoleucinate	ILE	130.17
	Proline	PRO	114.12
	Methioninate	MET	148.20
	Phenylalaninate	PHE	164.18
	Tryptophan	TRP	203.22
<hr/>			
	Serinate	SER	104.09
	Threoninate	THR	118.11
	Tyrosinate	TYR	180.18
	Cysteinate	CYS	120.15
	Asparaginate	ASN	131.11
	Glutamate	GLN	145.14
<hr/>			
	Aspartate	ASP	132.10
	Glutamate	GLU	146.12
<hr/>			
	Lysinate	LYS	145.18
	Arginate	ARG	173.19



Histidinate

HIS

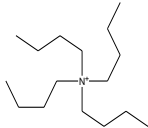
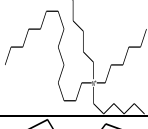
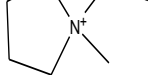
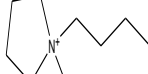
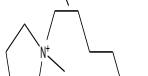


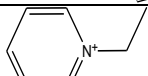

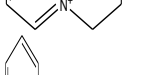

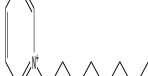
154.15

AA cations can be categorised into a few categories. Table 4 illustrates the cations used to design AAILs in this project. Phosphonium, ammonium and choline were chosen because they are the most common cations utilised in TSILs. Moreover, phosphonium and ammonium have a good CO₂ capture ability by chemisorption with long chain structures [20]. Choline cation is being focused on by many researchers nowadays as it is low in toxicity, anti-corrosion, and has higher CO₂ absorption

capability when reacting with AA anions [21,22]. Furthermore, the imidazolium absorption capacity of CO₂ is equimolar or less, according to the traditional cation, functionalised cation, and di-cation functionality [23]. Pyridinium is less expensive than imidazolium, and by increasing the number of alkyl chains, CO₂ absorption will increase [24]. The pyrrolidinium functional group was chosen because it is much less poisonous than the imidazolium functional group [25].

Table 4. Cations used for AAIL design in this study.

CATIONS				
Group	Structure	Name	Abbr.	MW (g/mol)
Phosphonium		Tetra-butyl phosphonium	P ₄₄₄₄	259.00
		Trihexyl(tetradecyl) phosphonium	P ₆₆₆₁₄	484.21
		3-aminopropyl-tributyl phosphonium	aP ₄₄₄₃	260.42
Choline		Choline	CH	104.17
Imidazolium		1-Ethyl-3-methylimidazolium	EMIM	111.17
		1-Butyl-3-methylimidazolium	BMIM	139.22
		1-Hexyl-3-methylimidazolium	HMIM	167.27
		1-Octyl-3-methylimidazolium	OMIM	195.32
		1-Decyl-3-methylimidazolium	C ₁₀ MIM	223.38
Ammonium		Tetramethylammonium	N ₁₁₁₁	74.14

		Tetrabutylammonium	N ₄₄₄₄	242.28
		Trihexyl(tetradecyl)ammonium	N ₆₆₆₁₄	466.00
Pyrrolidinium		1-Ethyl-1-methylpyrrolidinium	EMPYRR	114.21
		1-Butyl-1-methylpyrrolidinium	BMPYRR	142.26
		1-Hexyl-1-methylpyrrolidinium	HMPYRR	170.31
		1-Octyl-1-methylpyrrolidinium	OMPYRR	198.28
		1-Decyl-1-methylpyrrolidinium	C ₁₀ PYRR	226.25
Pyridinium		1-Ethylpyridinium	EPY	108.07
		1-Butylpyridinium	BPY	136.21
		1-Hexylpyridinium	HPY	164.27
		1-Octylpyridinium	OPY	192.32
		1-Decylpyridinium	C ₁₀ PY	220.21

RESULTS & DISCUSSION

This study aimed to investigate the CO₂ capture capacity of 440 AAILs by exploring the reactions of 22 cations, including phosphonium, choline, imidazolium, ammonium, pyrrolidinium, and pyridinium with varying numbers of alkyl chains and in combination with 20 AA anions, using COSMO-RS. A total of 7 properties were studied in COSMO-RS, which were σ -surface, σ -profile and σ -potential, the ideal activity coefficient, Henry constant, Gibbs free energy, CO₂ capacity, CO₂ selectivity, and performance index for all the 440 ILs. The chosen best-performance AAILs underwent a viscosity and ionic conductivity study in COSMO-RS. Moreover, interaction energy and bond distance were studied using the Tmolex and Pymol softwares.

Surface Charge Density/ σ -Surface

When DFT and COSMO-RS are used together, the appropriate electrostatics can be predicted with good accuracy. A DFT/COSMO-RS calculation gives us the total energy of a molecule in the self-consistent state in the conductor and the polarisation charge density, which even the conductor puts on the cavity to determine the electric field of the molecule [26]. It uses quantum chemical calculations to provide a 3D image of charge polarisation on the surface of molecules [16]. This polarisation charge density is a great way to describe the polarity on the surface of a molecule [26]. Various thermodynamic properties of molecules are determined using this polarisation charge density, which is represented in the graphical

function known as charge σ -profile and σ -potential later [16]. ILs with a lower molecular size will have a greater charge density and polarity, leading to increased solubility [15]. Representation of surface charge density/ σ -surface of the glutamate molecule as an example is given in Figure 3. Green represents neutral, blue represents positive, and red represents negative charges on the molecule.

To make it clear, glutamate molecules have a blue colour on the NH₂ bond, which is electropositive, red on the oxygen bond, which is electronegative, and green along the surface of the chain, which indicates neutrality. Moreover, all the σ -surface of cations and AA anions with minimum conformers were studied and are included in the **supplementary data**. By rotating one carbon atom along the connection connecting to other carbon atoms, isomers can exist in a variety of forms known as conformers. The minimum conformer is zero and is known as the most stable conformer which requires less energy and does

not have any steric hindrance or steric repulsion between the hydrogen bonds.

σ -Profile

In general, σ -profile emphasises the studied molecule's polarity. σ -profile and σ -potential comprise three major regions: hydrogen bond donor (H-D), non-polar, and hydrogen bond acceptor (H-A). The non-polar part is represented by the σ -value range -0.1 to 0.1 e.nm⁻², σ -values less than -0.1 describe the hydrogen bond donor region, while σ -values greater than +0.1 describe the hydrogen bond acceptor zone. The specific charge distribution on the molecule surface is related to the σ -profile. As the length of the alkyl chain increases, both the σ -peak values and non-polarity also increase accordingly [16], which will contribute significantly to the enhanced CO₂ absorption tendency. Representations of the σ -profile of the anions and cations used for AA-IL screening are illustrated in Figures 4 and 5.

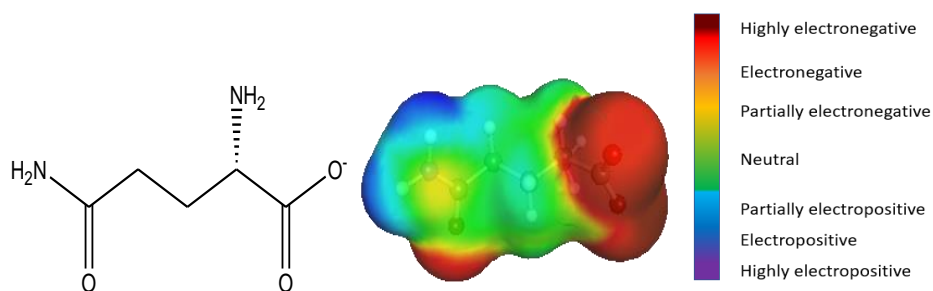


Figure 3. 2D structure and surface charge density of glutamate with colour indication.

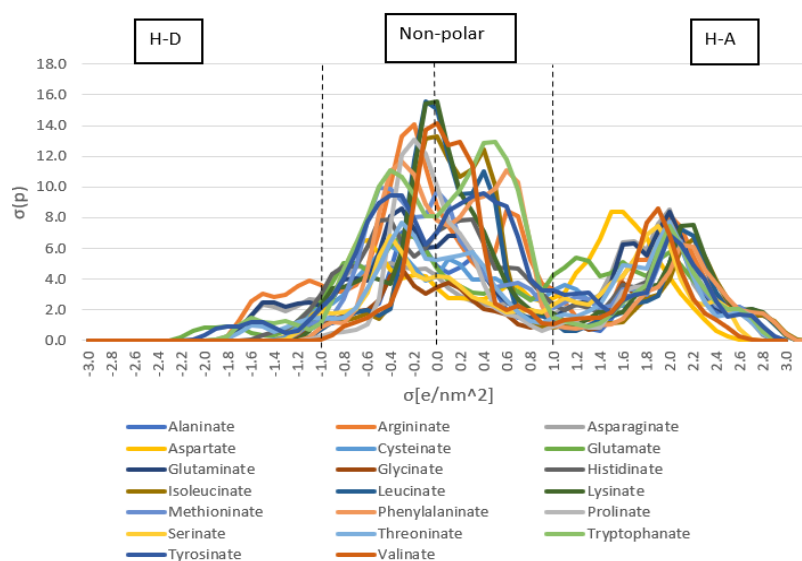


Figure 4. σ -profile of 20 AA anions studied in screening of AA-ILs.

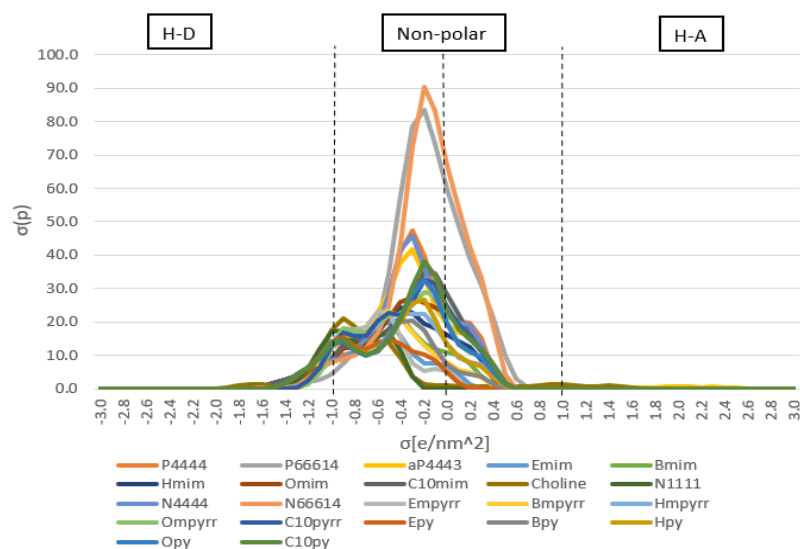


Figure 5. σ -profile of 22 cations studied in screening of AAILs.

The more non-polar (longer chain) cations react well with the highly polar (short chain) and more electronegative anions. Most of the anions are polar and the cations are highly non-polar. The anions, which are more electronegative, will attract well with H-A molecules, which in this case are electropositive cations. On the other hand, the electropositive cations could react with H-D molecules, which in this case is O⁻, an electronegative atom with a lone pair. This ionic interaction helps to form AAILs.

σ -Potential

A system's reactivity to a surface of polarity is measured by σ -potential, which focuses on how cations interact with AA-based anions [26]. In σ -potential, the non-polar part (σ -value range -0.1 to 0.1 e. nm⁻²) represents whether ILs are hydrophobic or hydrophilic. If $\mu(\sigma)$ is less than zero ($\mu(\sigma) < 0$), it is a hydrophilic interaction, and if $\mu(\sigma)$ is more than zero ($\mu(\sigma) > 0$), it is a hydrophobic interaction [14,26].

Figure 6 illustrates the σ -potential of [P₆₆₆₁₄] with twenty AA-based anions. The results below show that [P₆₆₆₁₄] had increasing interaction as a H-D. [P₆₆₆₁₄]'s interaction with twenty AA-based anions had larger negative-potentials ($\mu(\sigma)$) value ($\sigma < -0.1$ e/nm²), indicating a higher ability of the ILs to react with the H-D compound. The ($\mu(\sigma)$) values were slightly positive in the region of positive potential screening charge density ($\sigma > +0.1$ e/nm²), reflecting the absence of H-A surfaces in the ILs. These suggest that the intramolecular interaction between the specific cation and anions in the H-A was slightly weak, therefore it had a greater interaction with the H-D, and it was a more favourable interaction through

hydrophilic [27]. This phenomenon contributes to the stronger interaction of the (OH) functional group in [P₆₆₆₁₄] as a H-D with twenty AA-based anions, influenced by both the chemical structure and functional groups. The longer alkyl chains in [P₆₆₆₁₄] cation provided a larger surface area for interactions, while the functional groups facilitated hydrogen bonding with AA-based anions to form ILs.

Additionally, if ($\mu(\sigma)$) is negative in both negative and positive screening charge densities ($\mu(\sigma) < 0$), it indicates that the ILs may interact with both H-D and H-A molecules [16,27]. Whereas, if σ -potential values are positive ($\mu(\sigma) > 0$) in both negative and positive screening charge densities, it indicates that these ILs do not engage in polar interactions and prefer hydrophobic interactions [28]. All the other figures of σ -potential of the cations with twenty AA-based anions were studied and the results are included in the **supplementary data**. To conclude, all the AAILs are hydrophilic, which like water and can dissolve in water as well.

Henry's Constant

Based on the properties studied in COSMO-RS, the results below are the illustration of the prediction for the top 5 cations in CO₂ capture with 20 AA anions. All the other predicted AAIL results are included in the **supplementary data**.

The Henry's constant of each AAIL has been recorded to study the relationship between Henry's constant with CO₂ solubility and absorption capacity. The minimum value of the Henry's constant is 2.0 Mpa, which can increase the solubility of CO₂ in ILs.

If the Henry's constant value decreases, the solubility of CO₂ gas increases. The longer alkyl chain of the cation with more carbon chain length will lead to the

high solubility of CO₂ [28]. According to the results below, [P₆₆₆₁₄] and [N₆₆₆₁₄] have the lowest Henry's constant values.

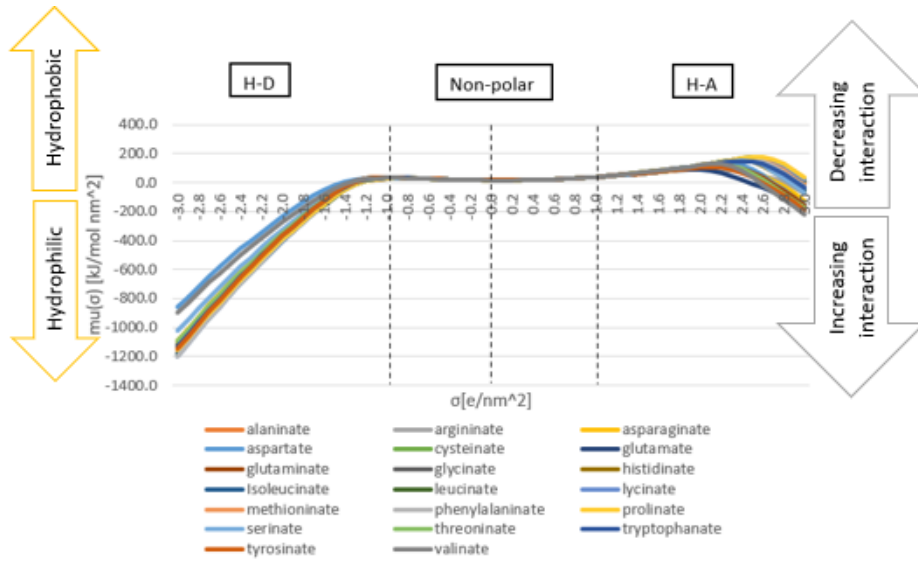


Figure 6. σ -potentials of [P₆₆₆₁₄] with twenty AA-based anions.

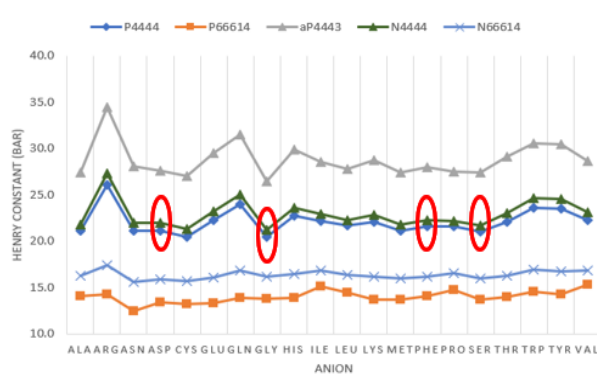


Figure 7. Henry's constants of CO₂ in top 5 cations with 20 AA-based anions at T=298.15 K and P=1 bar. *The AAILs identified with red circles represent the top performers in CO₂ capture as determined by this study.

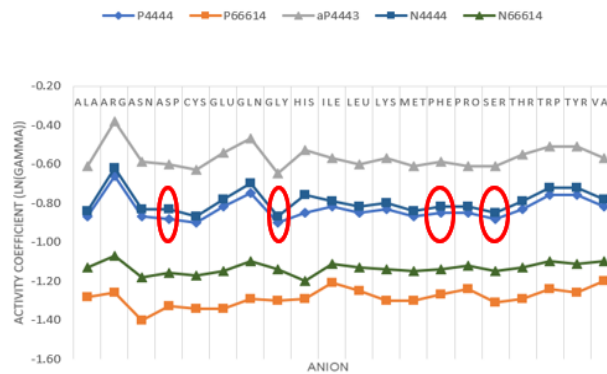


Figure 8. Activity Coefficients of CO₂ in top 5 cations with 20 AA-based anions at T=298.15 K and P=1 bar. *The AAILs identified with red circles represent the top performers in CO₂ capture as determined by this study.

Activity Coefficient

The activity coefficient is proportional to the solubility and interaction of unrelated substances. The lower the activity coefficient of a solute in a solvent, the higher the tendency of the solvent to interact with and absorb the solute [27]. According to the results in Figure 8, [P₆₆₆₁₄] and [N₆₆₆₁₄] have the lowest activity coefficient. For CO₂ solubility, especially in complex environments like AAILs, understanding and considering activity coefficients is essential for accurately predicting and describing the solubility behaviour of CO₂. The standard state of CO₂ in activity coefficient is 1 bar (atmospheric condition).

Gibbs Free Energy and Gibbs Solvation Free Energy

Gibbs free energy indicates the stability of ILs. The more negative the value, the more stable the ILs. According to the results in Figure 9, [P₆₆₆₁₄] and [N₆₆₆₁₄] have the most negative Gibbs free energy and Gibbs solvation free energy. The more stable ILs indicate that the interaction between cation-anion

will be weak, and the bond length will be longer so that more CO₂ can be captured by the ILs. Longer alkyl chains can provide additional van der Waals forces and hydrophobic interactions, leading to increased stability.

Gibbs free solvation energy is the amount of energy needed to dissolve CO₂ in a solvent [13]. The lower the solvation free energy and activity coefficient, the more effective the IL is for CO₂ extraction from other gases since it requires less energy. The negative solvation energy of the ammonium-based cation was greater than that of the other cations [13].

According to Henry's constant, activity coefficient, Gibbs free energy and Gibbs solvation energy, [P₆₆₆₁₄] and [N₆₆₆₁₄] cations show the best results in terms of capturing CO₂, which is tabulated in Figure 10. Then, followed by [N₄₄₄₄] and [P₄₄₄₄] cations. Even though the [aP₄₄₄₃] cation has better Gibbs energy and solvation energy compared to [P₄₄₄₄] and [N₄₄₄₄], it shows the highest value in terms of Henry's constant and activity coefficient according to the results above.

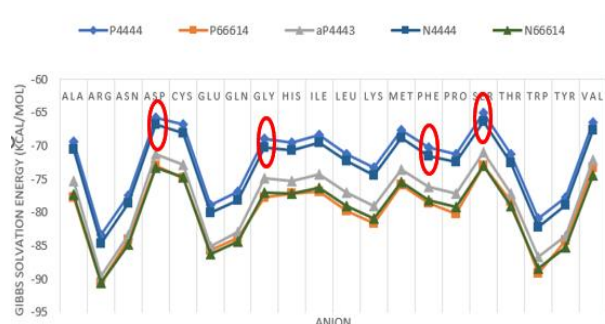


Figure 9. The Gibbs free energy of ILs in top 5 cations with 20 AA-based anions at T=298.15 K and P=1 bar. *The AAILs identified with red circles represent the top performers in CO₂ capture as determined by this study.

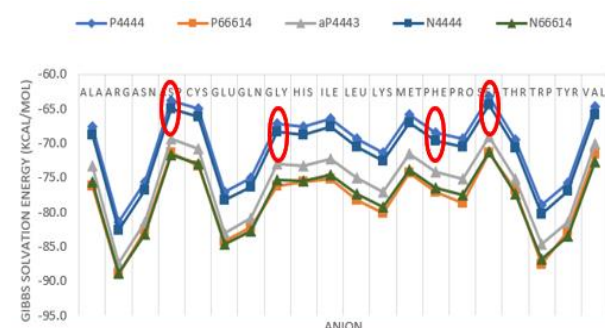


Figure 10. The Gibbs free solvation energy of CO₂ in top 5 cations with 20 AA-based anions at T=298.15 K and P=1 bar. *The AAILs identified with red circles represent the top performers in CO₂ capture as determined by this study.

The Gibbs free solvation energy measures the energy change associated with the process of solvating one mole of a substance in a particular solvent. The Gibbs free solvation energy (ΔG_{solv}) is defined by Equation 4 below:

$$\Delta G_{\text{solv}} = \Delta H_{\text{solv}} - T\Delta S_{\text{solv}} \quad (\text{Equation 4})$$

- ΔH_{solv} is the enthalpy change of solvation (positive if energy is absorbed, negative if energy is released).
- ΔS_{solv} is the entropy change of solvation.
- T is the absolute temperature, 298.15 K.

If ΔG_{solv} is negative, it indicates a spontaneous and energetically favourable solvation process. The Gibbs solvation energy of -90 kcal/mol suggests that when CO₂ dissolves in AAIL, it releases a significant amount of energy, making the process favourable.

CO₂ Capacity

Figures 11, 12 and 13 show the CO₂ capacity, which is defined as the absorption capability of CO₂ in ILs.

Capacity also determines the number of ILs needed for the removal of CO₂ by extraction [15]. The higher the capacity, the fewer ILs are needed to remove CO₂ and the better the CO₂ capture capacity.

Hence, [P₆₆₆₁₄] and [N₆₆₆₁₄] have the better Henry constant, activity coefficient, Gibbs free energy, and capacity compared to any other ILs. Henry constant, activity coefficient, and Gibbs free energy should be directly proportional to each other.

Selectivity

Selectivity was calculated in terms of CO₂ /N₂ and CO₂/O₂. The higher the selectivity, the better ILs performance or gas solubility [18]. Figures 14 and 15 show that [P₆₆₆₁₄] and [N₆₆₆₁₄] have the lowest selectivity as their absorption capacity is higher in all the gases (CO₂, N₂, and O₂), which means they absorb all gas components including CO₂, N₂, and O₂. But [P₄₄₄₄] and [N₄₄₄₄] show better selectivity as the capacity of CO₂ is higher than the other 2 gases (N₂ and O₂), which is good as we targeted to capture CO₂.

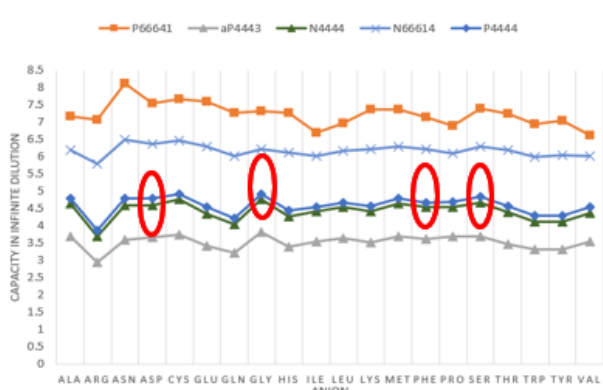


Figure 11. CO₂ capacity in infinite dilution of CO₂ in top 5 cations with 20 AA-based anions at T=298.15 K and P=1 bar.

*The AAILs identified with red circles represent the top performers in CO₂ capture as determined by this study.

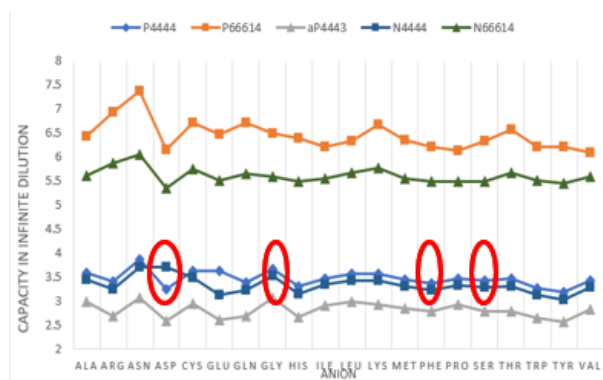


Figure 12. CO₂ capacity in infinite dilution of N₂ in top 5 cations with 20 AA-based anions at T=298.15 K and P=1 bar.

*The AAILs identified with red circles represent the top performers in CO₂ capture as determined by this study.

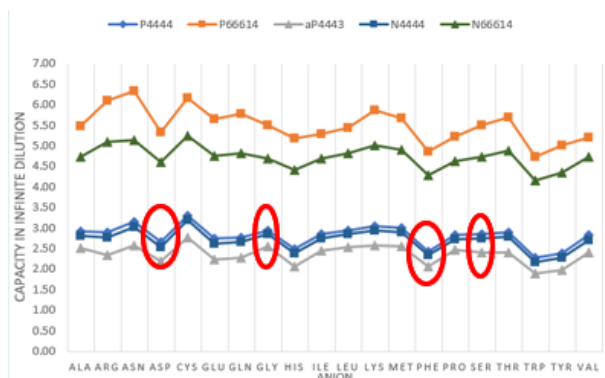


Figure 13. CO₂ capacity in infinite dilution of O₂ in top 5 cations with 20 AA-based anions at T=298.15 K and P=1 bar.

*The AAILs identified with red circles represent the top performers in CO₂ capture as determined by this study.

The chain length of the cations, such as [P₆₆₆₁₄] and [N₆₆₆₁₄], in ILs influences their selectivity for CO₂ capture. ILs with longer alkyl chains tend to have increased hydrophobicity and reduced polarity [29]. As a result, they exhibit weaker interactions with polar molecules like CO₂, N₂, and O₂. This weaker interaction leads to lower selectivity, as these ILs may absorb all gas components indiscriminately, rather than prioritising CO₂ capture.

Conversely, reference [13] states that ILs with shorter alkyl chains typically have higher polarity and stronger interactions with polar molecules. This increased polarity enables them to selectively absorb CO₂ over other gases, like N₂ and O₂. Therefore, ILs with shorter alkyl chains, such as [P₄₄₄₄] and [N₄₄₄₄], demonstrate better selectivity for CO₂ capture.

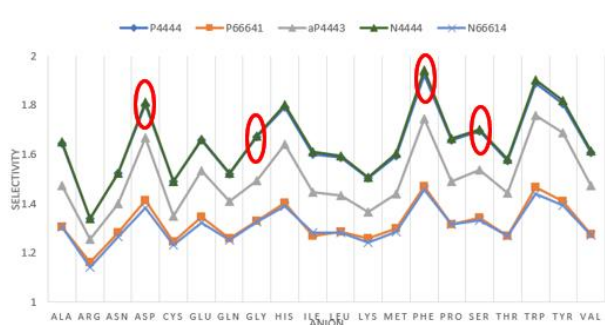


Figure 14. The selectivity of CO₂/N₂ in top 5 cations with 20 AA-based anions at T=298.15 K and P=1 bar.

*The AAILs identified with red circles represent the top performers in CO₂ capture as determined by this study.

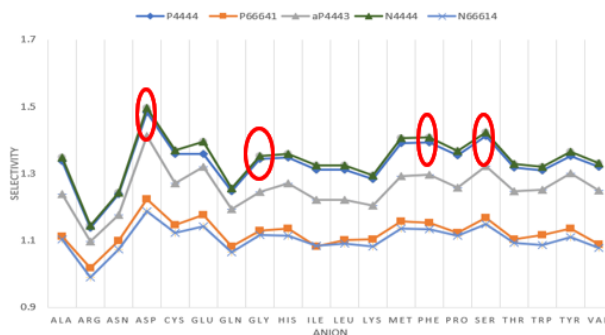


Figure 15. The selectivity of CO₂/O₂ in top 5 cations with 20 AA-based anions at T=298.15 K and P=1 bar.

*The AAILs identified with red circles represent the top performers in CO₂ capture as determined by this study.

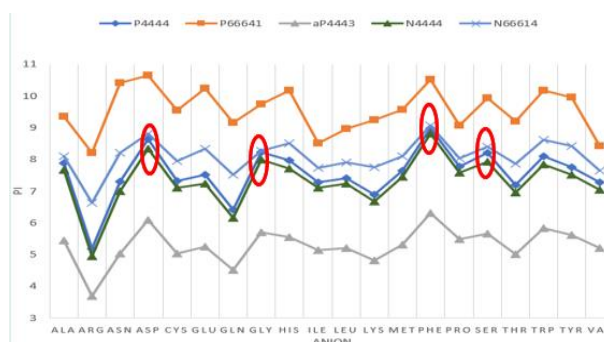


Figure 16. Results of performance index of CO₂/N₂ with the capacity of CO₂ for top 5 cations with 20 amino acid-based anions.

*The AAILs identified with red circles represent the top performers in CO₂ capture as determined by this study.

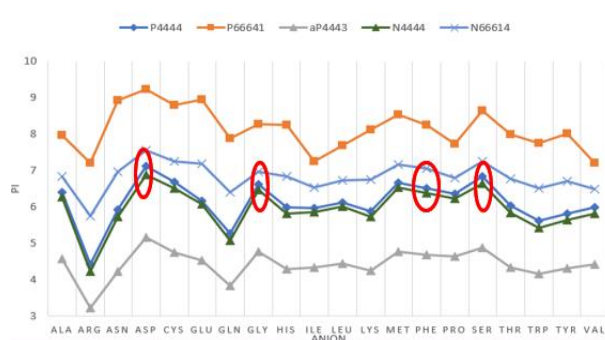


Figure 17. Results of performance index of CO₂/O₂ with capacity of CO₂ for top 5 cations with 20 amino acid-based anions.

*The AAILs identified with red circles represent the top performers in CO₂ capture as determined by this study.

Performance Index

Figures 16 and 17 show the performance index (PI), which assesses the performance and efficacy of any solvent in accomplishing the absorption or extraction of CO₂. PI is the product of any solvent's selectivity and capacity at infinite dilution [15]. The higher the PI, the higher the performance of ILs. [P₆₆₆₁₄] and [N₆₆₆₁₄] have the highest performance index compared to others.

Chosen ILs with High Performance in CO₂

The trendline for all the cations with 20 amino acid anions looks the same but when observed closely, the results of the anions vary slightly with various cations. Usually for carbon capture, the important properties that need to be taken into consideration are the Henry constant, activity coefficient, and PI. PI is the key point which helps to choose the best-performance ILs. For gas capture application, it is important to choose the ILs based on the Henry constant as well. From the results above, the cations of [P₆₆₆₁₄] and [N₆₆₆₁₄] had the highest performance compared to all the other cations, but for this study, [P₄₄₄₄] and [N₄₄₄₄] with the second highest performance were chosen because of low cost to synthesis compared to [P₆₆₆₁₄] and [N₆₆₆₁₄].

Hence, the top 8 ILs consist of 2 cations ([P₄₄₄₄] and [N₄₄₄₄]) and 4 anions (Aspartate [ASP], Glycinate [GLY], Serinate [SER] and Phenylalaninate [PHE]), with better-predicted results in CO₂ capture. The ILs were chosen based on PI and the results were compared with Henry's constant and activity coefficient to finalise the ideal best performance ILs in CO₂ capture.

Single sites in ILs can yield up to a 1:1 stoichiometry absorption capacity. While multiple sites might not even result in doubled capacity. The efficiency of a site may be reduced when numerous sites share a single negative charge. Moreover, due to the complicated interactions in ILs, even if two sites are independent or each has a negative charge, the absorption capacity may not double [8]. Therefore, it is obvious from the results that the anions with only one active site, [ASP], [GLY], [SER], and [PHE], performed better than those with more active sites.

Protonation constant (pK_a) is an important physiochemical characteristic for AAs that aids in the analysis of reaction processes and molecular structures in aqueous solutions. The AAs had high pK_a values ranging from 8 to 10, like normal alkanol amine solutions (which have NH₂ and OH). This suggests

that the presence of the main amine group in AA solutions enabled it to react with CO₂ with considerable chemical reactivity. pH indicates the acidity or basicity of a solution, whereas p*K*_a measures the strength of an acid or a base (tendency to dissociate in an aqueous solution). Because of the diverse chemical forms of AAs, variation in pH value may affect adsorbent performance. The adsorbents produced at pH 5 had greater adsorption capabilities than those made at pH 7. When reacting with acidic CO₂ molecules, alkaline pH is generally preferred. AAs are made up of amino groups, primarily amine (-NH₂) and carboxyl (-COOH) groups with a general R-side chain in the structure, which aids in CO₂ capture by chemical adsorption (chemisorption) [30]. Table 5 shows the molecular weights and p*K*_a values

of 20 AAs which have been highlighted in a previous article [30].

A lower MW amine-modified CO₂ adsorbent displayed a somewhat greater CO₂ absorption than a high MW adsorbent. Due to equivalent amino functional groups that contribute to high adsorption capacity, a similar trend is predicted for AA-based adsorbents. This statement is also supported by reference [31] which summarise that the reduced CO₂ adsorption capacity observed in an amine with a large molecular weight is likely attributed to the presence of fewer active adsorption sites in the sample. As a result, among the 20 basic AAs, [GLY] with the lowest MW (75.07 g/mol) is estimated to be the best in capturing CO₂ [30].

Table 5. Molecular weights and p*K*_a values of 20 basic amino acids [30].

Amino Acid	Molecular weight, MW (g/mol)	p <i>K</i> _a
Alanine	89.1	10.01, 9.87
Arginine	174.2	12.48, 9.04
Asparagine	132.12	8.80
Aspartic acid	133.11	10.16, 9.60
Cysteine	121.16	8.18
Glutamic acid	147.13	9.97, 9.67
Glutamine	146.15	9.13
Glycine	75.07	9.77, 9.78
Histidine	155.16	9.33
Isoleucine	131.18	9.68
Leucine	131.18	9.75
Lysine	146.19	10.67, 8.95
Methionine	149.21	9.2, 9.21
Phenylalanine	165.19	9.29, 9.31
Proline	115.13	10.76, 10.6
Serine	105.09	9.15
Threonine	119.12	9.12
Tryptophan	204.23	9.39
Tyrosine	181.19	9.11
Valine	117.15	9.72

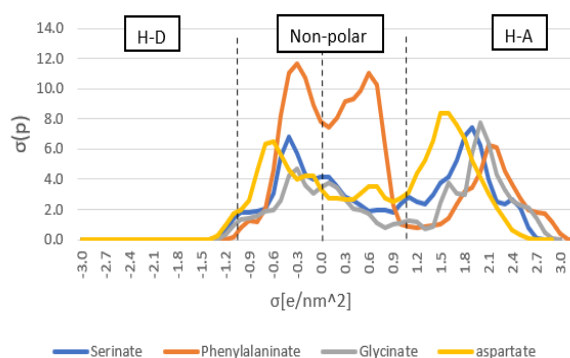


Figure 18. Sigma profiles for 4 chosen anions.

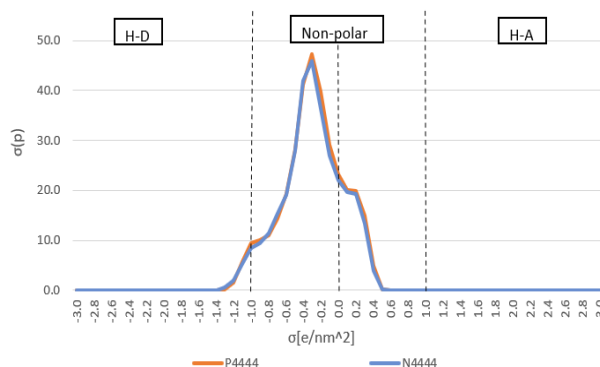


Figure 19. Sigma profiles for 2 chosen cations.

The stronger the polarity, the greater the CO₂ capture. On the other hand, acidic AAs include carboxyl groups in their side chains and have low pK_a values that tend to lose protons, resulting in a negative charge. These AAs are [ASP] and glutamic acid [GLU] [30]. To summarise, [GLY] and [PHE] are in a non-polar group, but [ASP] and [SER] are in a polar group. According to the sigma profile, [GLY], [ASP], and [SER] are less non-polar (higher polarity) and tend to absorb more CO₂. Except for [PHE], all the other 3 chosen anions are more electronegative (which will highly react with hydrogen acceptors). [PHE] has better performance because it has a low pK_a value and a longer chain of anion which tends to absorb more CO₂. Figures 18 and 19 below illustrate the sigma profiles of the chosen anions and cations.

The selection of [P₄₄₄₄] and [N₄₄₄₄] cations was based on considerations of cost-effectiveness and selectivity. Although [P₆₆₆₁₄] and [N₆₆₆₁₄] demonstrate higher CO₂ capture capacity, but their higher cost and poor selectivity render them less favourable options for this study. On the other hand, increasing the alkyl chain of phosphonium also causes a slightly poisonous effect on marine bacteria [32]. Therefore, the third and fourth highest performance cations were chosen from the COSMO-RS result, which were [N₄₄₄₄] and [P₄₄₄₄].

From the sigma profile, more polar and electronegative AA anions paired with highly non-polar and increasing alkyl chain cations showed better performance in CO₂ capture [17]. The anion and cation would be further apart because of the increasing length of the alkyl chain. According to the COSMO-RS findings, ILs with longer alkyl chains exhibit more negative Gibbs free energy, which indicates greater stability and enhanced solubility for CO₂. This phenomenon arises because when the anion and cation are situated farther apart, their interaction decreases, resulting in more available free volume within the ILs [14]. Therefore, it is easy for CO₂ to be inserted into the free volume (free space).

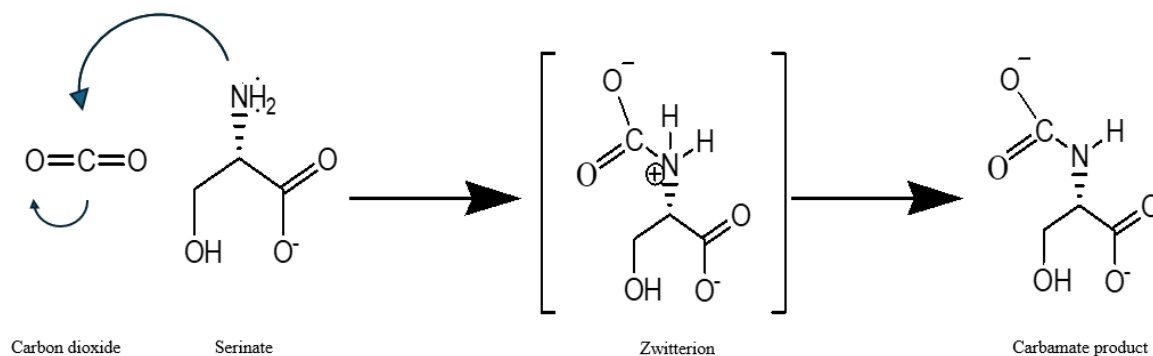
In this case, the anion is the one that captures CO₂. Hence, the CO₂ insertion into the free volume tends to have higher interaction with the NH₂ functional group in the anion due to the presence of a lone pair [33]. This is why the longest-chain cation has the highest CO₂ capture or solubility compared to the short-chain cations. Figure 20 shows the mechanism of CO₂ capture by the anion (serinate). In the initial reaction pathway, an anion of AAILs reacts with CO₂ to generate a zwitterionic intermediate. Subsequently, in the second step, this zwitterion undergoes proton transfer to yield carbamate products [34].

Thus, the chosen 2 cations would be paired with all 4 anions to produce the respective ILs as shown in Table 6.

Viscosity and Ionic Conductivity

Viscosity and ionic conductivity were also predicted using COSMO-RS. Chain pliability, van der Waals interaction potency, and the tendency for hydrogen bond formation all affect viscosity. The quantity and mobility of charge carriers are the primary determinants of conductivity. The poor conductivities of the ILs might be attributed to the charge carriers' limited movement, which is induced by a high number of hydrogen-bonding interactions [35].

The longer chain of the cation causes an increase in the number of van der Waals (weak) interactions and an increase in the number of hydrogen bond interactions leads to higher viscosity and decreasing rate of ion mobility of the salts, which leads to decreasing ionic conductivity [35,36]. The increasing chain length of the AA anion also will increase the viscosity [37]. According to the literature, AAILs with longer alkyl chains, such as [P₄₄₄₄] and [N₄₄₄₄], exhibit high viscosity and low conductivity at ambient temperature. Both cations have longer flexible chains and high molecular weight. Chiral AAILs exhibit low ionic conductivities, low ion mobility, higher viscosities, and higher melting points. The viscosity of AAILs limits many of their possible uses for fluid and electrolyte materials [36].

**Figure 20.** Mechanism of CO₂ capture by an anion [34].**Table 6.** Selected high-performance ILs from COSMO-RS.

CATIONS	ANIONS
Tetrabutylphosphonium	Phenylalanine
	Aspartic acid
	Glycine
	Serine
Tetrabutylammonium	Phenylalanine
	Aspartic acid
	Glycine
	Serine

The geometry of AA anions also has a significant impact on the viscosity of AAILs [35,38]. The viscosity of anions will increase with more complicated structures. Viscosity determines electric conductivity [38]. Especially in the case of AAs as anions, the majority of them contain functional groups such as carboxyl, hydroxyl, and so on. This means that there is some intra- and intermolecular interactions. In other words, the addition of functional groups such as an H-bonding donor or acceptor enhances viscosity while decreasing ionic conductivity via intra/intermolecular interactions [36].

According to the COSMO-RS results, the viscosity increases in the order of: [SER] < [ASP] < [GLY] < [PHE]. Figure 21 shows the viscosity of the AAILs. Supposedly, according to the experimental results of previous works summarised in Table 7, the increasing viscosity should be in the order of: [GLY] < [SER] < [PHE] < [ASP]. The discrepancies observed between the results obtained from COSMO-RS simulations and experimental data from previous studies can be attributed to the limitations of the COSMO-RS software. Unlike experimental measurements, COSMO-RS simulations do not fully account for the interactions between the cation and anion ILs. Therefore, the viscosity and ionic conductivity results obtained from COSMO-RS should be regarded as indicative rather than definitive, as the simulations primarily focus on the molecular structure. Table 7 in this study includes the reported optimal viscosity

range from previous research, providing valuable context for interpreting the results.

Due to the fact that [Asp] has two carboxyl groups in the alkyl chain, the effect of the carboxyl group (-COOH) insertion is substantially greater than that of the amino and hydroxy groups (-OH). When ions have the capability of having ion-ion interactions via hydrogen bonding along with electrostatic force, their solution characteristics are poorer than those of ions with no functional groups [39]. [ASP] is more viscous compared to [SER] because the carboxylic group is more acidic and stronger compared to the hydroxyl group as it has strong intermolecular forces and hydrogen bonding interactions [14]. [ASP] contains a (COOH) group which is hydrophilic, and it can promote hydrogen bonding interactions with surrounding molecules which increases the viscosity by enhancing intermolecular forces.

[PHE] showed the second highest viscosity due to the bigger size of the anion and the possibility of pi-pi interaction with the aromatic ring, which causes the high viscosity [36]. The aromatic ring in [PHE] is hydrophobic and tends to decrease the ability of a molecule to form a strong hydrogen bonding with another molecule, even if it has a stronger van der Waals interaction.

Besides that, the lowest viscosity was found in [GLY] [39]. In terms of solubility, [GLY] has higher CO₂ solubility due to smaller MW [30]. This is due to

the smaller molecular weight and a simple molecular structure. [SER] is more viscous compared to [GLY] due to the presence of a (-OH) bond in the alkyl chain which also has higher hydrogen bond interactions than

[GLY]. Therefore, the ionic conductivity would be in an increasing order of: [ASP] < [PHE] < [SER] < [GLY]. Higher viscosity would also lead to low diffusion of CO₂ into the AAILs.

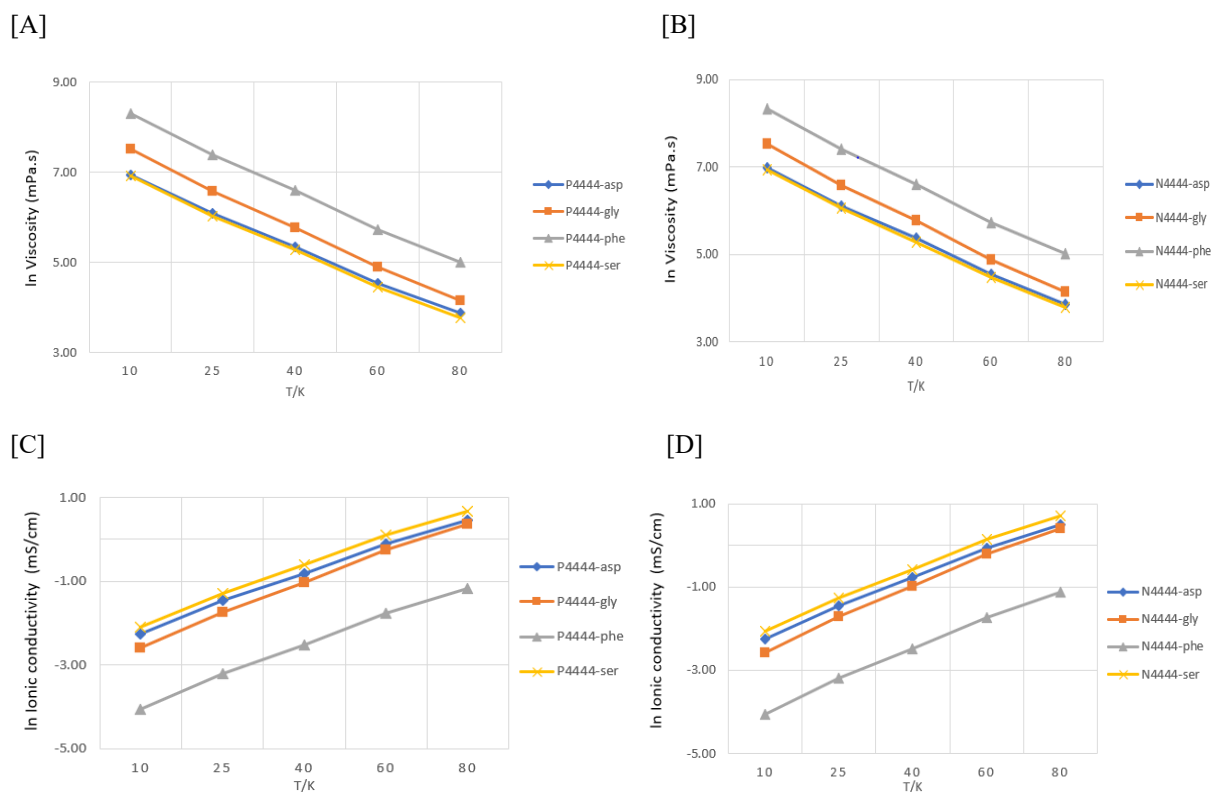


Figure 21. Predicted viscosity of (A) [P₄₄₄₄] and (B) [N₄₄₄₄]; predicted ionic conductivity of (C) [P₄₄₄₄] and (D) [N₄₄₄₄] (with [PHE], [ASP], [SER] and [GLY]).

Table 7. Predicted results from COSMO-RS and results from previous works and experiments.

AAILs	Predicted ionic conductivity at 25°C (mS/cm)	Predicted viscosity at 25°C (mPa.s)	Viscosity from previous work at 25°C (mPa.s)
[P ₄₄₄₄][SER]	0.275	419.89	734.20 [35], 902 [39]
[P ₄₄₄₄][ASP]	0.230	441.42	7437 [39]
[P ₄₄₄₄][GLY]	0.176	720.54	232.85 [35], 415 [39]
[P ₄₄₄₄][PHE]	0.040	1603.59	927 [39]
[N ₄₄₄₄][SER]	0.284	424.11	-
[N ₄₄₄₄][ASP]	0.237	450.34	-
[N ₄₄₄₄][GLY]	0.183	727.78	-
[N ₄₄₄₄][PHE]	0.041	1635.98	-

From the results above, it can be summarised that if the viscosity increases, the ionic conductivity will decrease due to low ion mobility. Table 7 shows the predicted viscosity and ionic conductivity results from COSMO-RS and the experimental viscosity results from previous works. The predicted results of [P₄₄₄₄] and [N₄₄₄₄] are more or less the same.

Density Functional Theory (DFT)

The usual benefit of ILs over other solvents is their extremely low vapour pressure and chemical composition, which may be modified to make them more effective for particular purposes. Both physisorption and chemisorption may be used by ILs to absorb CO₂, with the latter method frequently having a higher performance. By including amino groups in their molecular components, the ILs can achieve CO₂ chemisorption by allowing their interaction with CO₂ to produce carbamates or carbamic acids [33].

Both CO₂-anion and cation-anion interactions have a significant impact on the solubility of CO₂ in physisorption. IL and CO₂ interact non-covalently through electrostatic and van der Waals interactions, which are the basis for physisorption. The benefit of physisorption is that, due to the comparatively low absorption enthalpy, less energy is needed during the desorption process. However, the absorption capacity can be restricted by the CO₂ solubility. Although physisorption may be enough for CO₂ separation, the absorption capacity at atmospheric pressure remains limited for sorbent applications, which led to the development of TSILs for CO₂ chemisorption [40].

In chemisorption, the basicity of the anion may be utilised to modify the reactivity with CO₂, and the cation can be modified to increase the stability of the IL. Functionalised anions were developed to increase the absorption capacity. A 1:1 stoichiometry for the AAILs' absorption is possible. Carbamic acid is created when CO₂ and AAs combine. A previously published article mentions that tethering an amine group to the cation favours the formation of zwitterion, a carbamate product, whereas tethering an amine group to the anion results in the formation of carbamic acid, involving only one amine group, due to the instability of the formation of a dianion [40].

A more negative value indicates that the Interaction energy (IE) is higher. When the IE between CO₂-ILs is higher (strong attraction), the IE between cation-anion should be lower (weak attraction). Theoretically, the lower IE between the cation-anion shows that the distance between the cation-anion is longer, more free volume is present and the solubility of gas will be higher [14]. Therefore, more CO₂ can be captured by the ILs, and it shows a higher IE between CO₂-ILs. In simpler terms, phosphonium-based ILs exhibit slightly higher IE compared to ammonium-based ILs, although the differences between the two are minimal. But other factors also need to be taken into consideration as they can affect the result. Table 8 summarise the interaction energy and the bond length of phosphonium and ammonium-based ILs.

The interaction energy (IE) of ILs-CO₂ was predicted based on Equation 5 and the interaction energy (IE) of cation-anion was predicted based on Equation 6 [35].

$$\Delta E_{(\text{cation-anion})} = E_{(\text{cation-anion ion pair})} - [E_{(\text{cation})} + E_{(\text{anion})}] \quad (\text{Equation 5})$$

$$\Delta E_{(\text{ILs-CO}_2)} = E_{(\text{ILs-CO}_2 \text{ ion pair})} - [E_{(\text{cation})} + E_{(\text{anion})} + E_{(\text{CO}_2)}] \quad (\text{Equation 6})$$

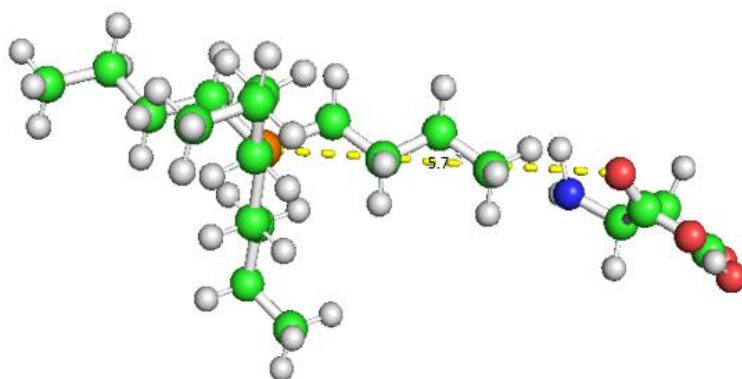
Table 8. Interaction energy and bond length of phosphonium and ammonium-based ILs.

Entry	AAILs	Interaction energy, IE (kcal mol ⁻¹)		The bond length of cation-anion (Å)	The length of anion- CO ₂ (Å)
		Cation-anion (Eq 5)	ILs-CO ₂ (Eq 6)		
1	[P ₄₄₄₄] [GLY]	0.072	-0.139	6.6	1.9
2	[P ₄₄₄₄] [SER]	0.001	-1.193	6.2	2.2
3	[P ₄₄₄₄][PHE]	-0.006	-0.061	6.0	2.2
4	[P ₄₄₄₄][ASP]	-1.016	-1.144	5.7	2.7
5	[N ₄₄₄₄] [GLY]	0.065	-0.132	6.1	2.0
6	[N ₄₄₄₄] [SER]	0.000	-0.075	5.8	2.2
7	[N ₄₄₄₄][PHE]	-0.001	-0.141	5.0	2.4
8	[N ₄₄₄₄][ASP]	-1.004	-1.132	4.3	2.8

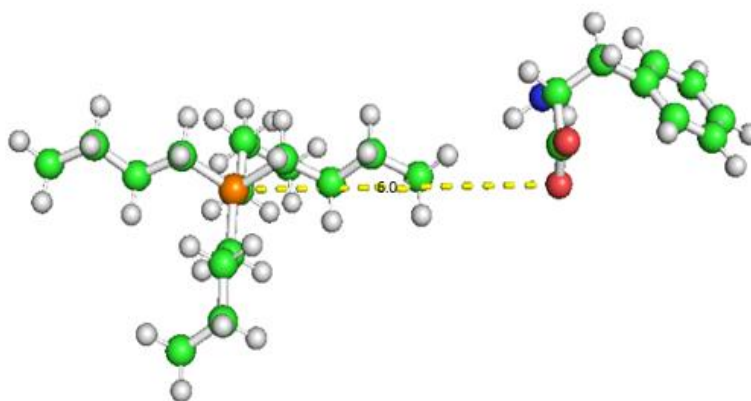
Interaction energy was calculated using potential energy generated during structure optimisation using the Turbomole software and bond length was determined in the Pymol software. According to a previously published article, [BMIM][GLY] has a larger or stronger interaction energy than [BMIM][VAL]. They emphasised that this behaviour may be caused by the [BMIM][VAL] having a longer alkyl chain, which increases the steric barrier towards CO₂ sorption. The formation of carbamic acid occurs when CO₂ gas is absorbed onto the nitrogen atom (N) within the AA chain, leading to the sorption of CO₂ onto AAILs. Carboxylate anions present in AAILs possess a high attraction for the cation's hydrogen atom [41]. As the N and O atoms in these IL anions have no direct connections to the hydrogen atoms, intermolecular hydrogen bond interaction is considerably reduced, which also reduces viscosity. Due to the complete use of the electronegative N and O atoms for CO₂ absorption, these ILs exhibit significant absorption capabilities [42].

Another approach to conceptually explain the behaviour of ILs and solutes is molecular modelling. Using the DFT approach, all 8 ILs and ILs-gas

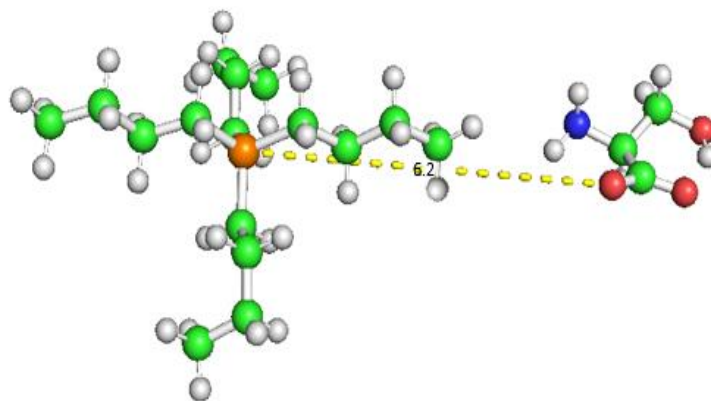
complexes were optimised. The most stable AAIL structures are shown in Figures 22 and 23. The solubility of CO₂ can be described by hydrogen bond interaction using the optimised geometry. As can be seen, hydrogen bonds formed between the P⁺, N⁺ or H atom of the cations and (-COO) group of the AA anions. CO₂ formed bonds with the (-NH) group of AA anions. Covalent bonds with atoms like C, N, and P that are less electronegative could be categorised as hydrogen bond donors. Additionally, to form hydrogen bonds, the proton donor must be slightly polar to allow for the formation of a direct contact that is equivalent to hydrogen bonds. As a result, it may be said that any covalent bond between (-COO) groups of AA anions and hydrogen in the cations forms a hydrogen bond [14,43,44,45]. Normally, the interaction between cation-anion in DFT will follow the H-bond interaction. More electronegative atoms in an anion (-COO) will interact with electropositive atoms in the cation. In this study, the sequence of hydrogen bond strength decreases (bond length cation-anion increases) in the order of [P₄₄₄₄][ASP] < [P₄₄₄₄][PHE] < [P₄₄₄₄][SER] < [P₄₄₄₄][GLY]; followed by [N₄₄₄₄][ASP] < [N₄₄₄₄][PHE] < [N₄₄₄₄][SER] < [N₄₄₄₄][GLY].



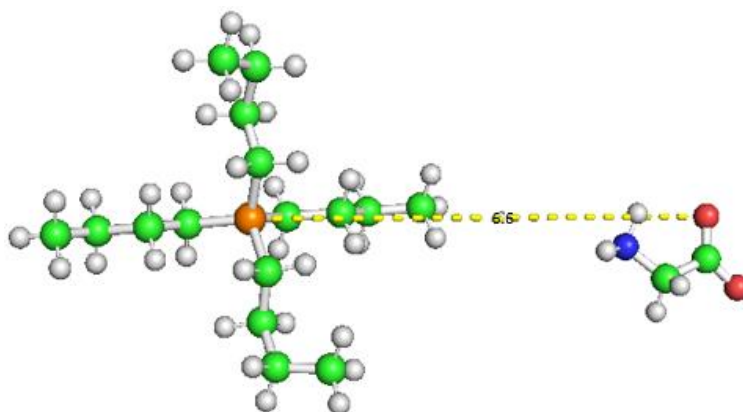
(A) [P₄₄₄₄][ASP] (bond length in Å of cation-anion, 5.7)



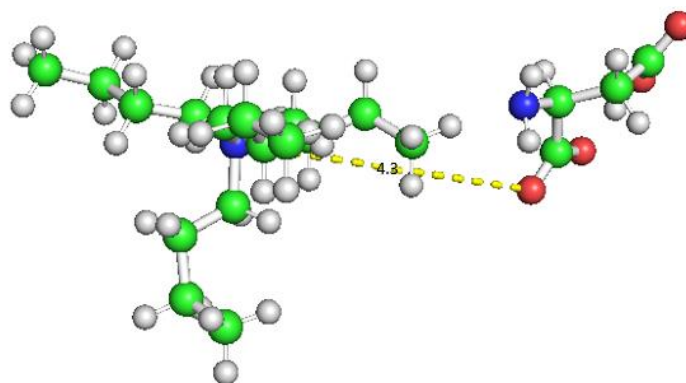
(B) [P₄₄₄₄][PHE] (bond length in Å of cation-anion, 6.0)



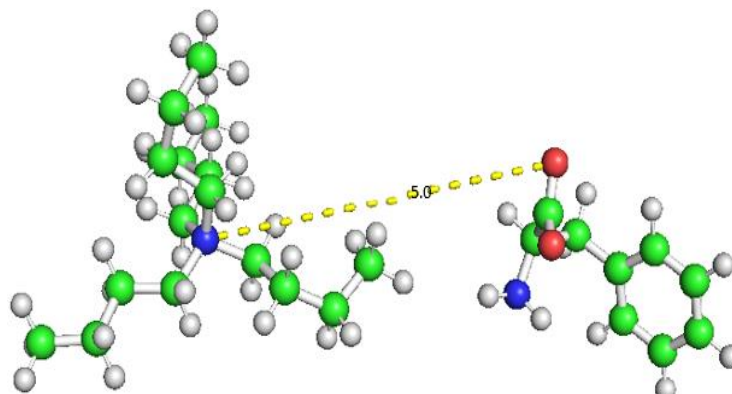
(C) [P₄₄₄] [SER] (bond length in Å of cation-anion, 6.2)



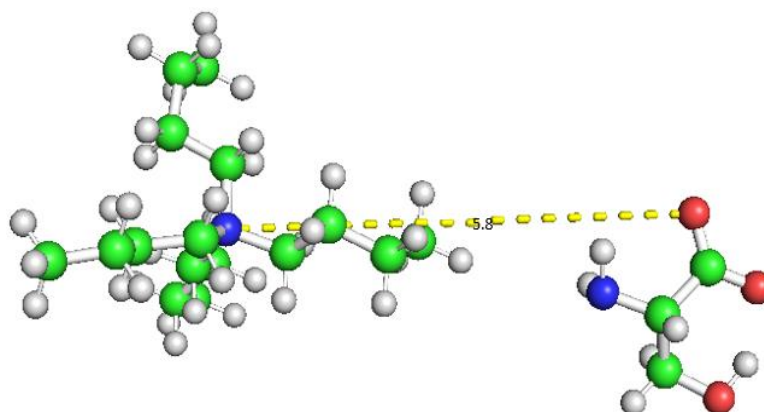
(D) [P₄₄₄] [GLY] (bond length in Å of cation-anion, 6.6)



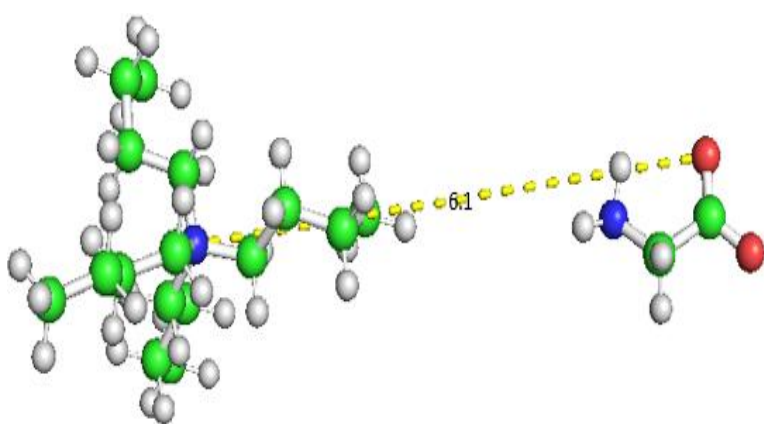
(E) [N₄₄₄] [ASP] (bond length in Å of cation-anion, 4.3)



(F) [N₄₄₄] [PHE] (bond length in Å of cation-anion, 5.0)

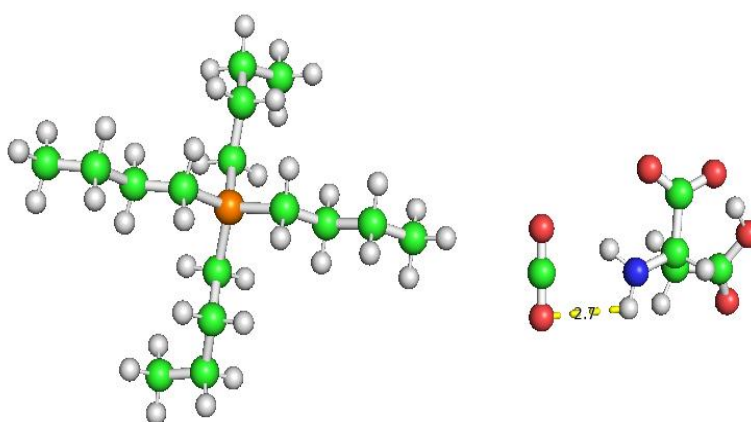


(G) [N₄₄₄₄] [SER] (bond length in Å of cation-anion, 5.8)

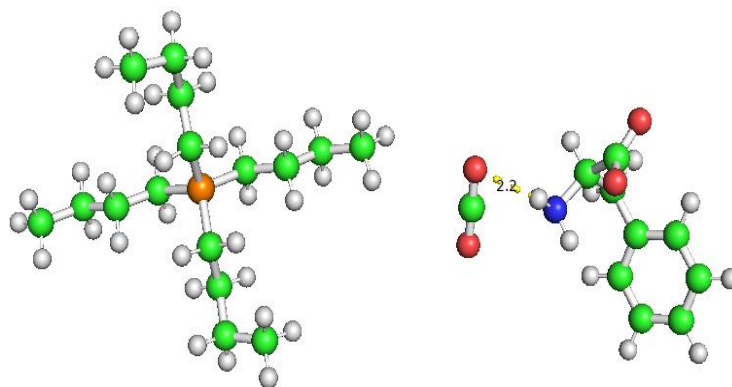


(H) [N₄₄₄₄] [GLY] (bond length in Å of cation-anion, 6.1)

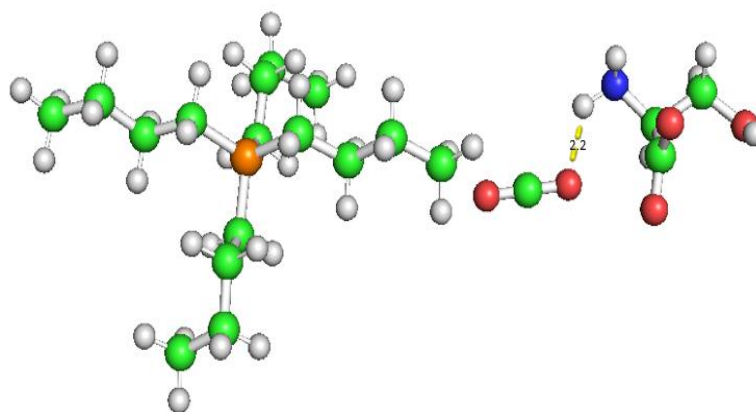
Figure 22. Optimised structures of 8 AAIL (cation + anion) complexes, which are (A) [P₄₄₄₄] [ASP], (B) [P₄₄₄₄] [PHE], (C) [P₄₄₄₄] [SER], (D) [P₄₄₄₄] [GLY], (E) [N₄₄₄₄] [ASP], (F) [N₄₄₄₄] [PHE], (G) [N₄₄₄₄] [SER], and (H) [N₄₄₄₄] [GLY].
* Bond between (P⁺) or (N⁺) atom in cation attached with (COO⁻) group in anion.



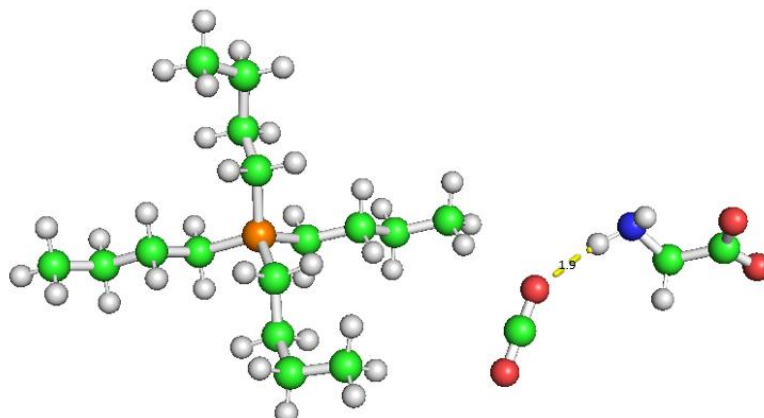
(A) [P₄₄₄₄] [ASP]-CO₂ (bond length in Å of anion-CO₂, 2.7)



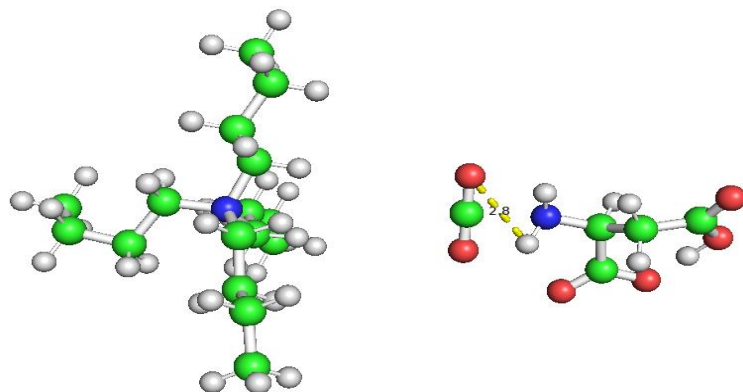
(B) [P₄₄₄₄] [PHE]-CO₂ (bond length in Å of anion-CO₂, 2.2)



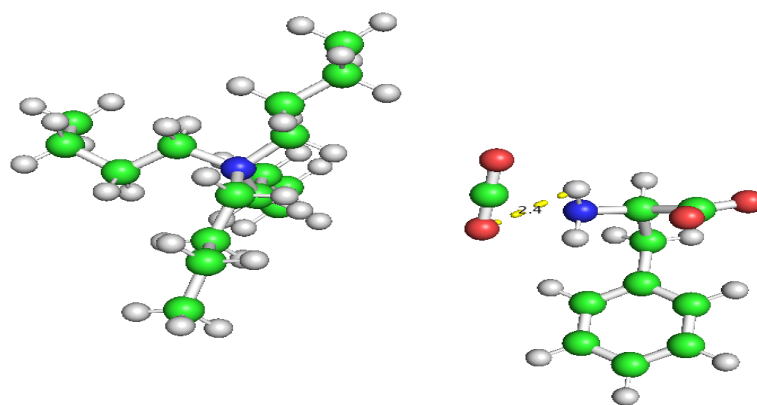
(C) [P₄₄₄₄] [SER]-CO₂ (bond length in Å of anion-CO₂, 2.2)



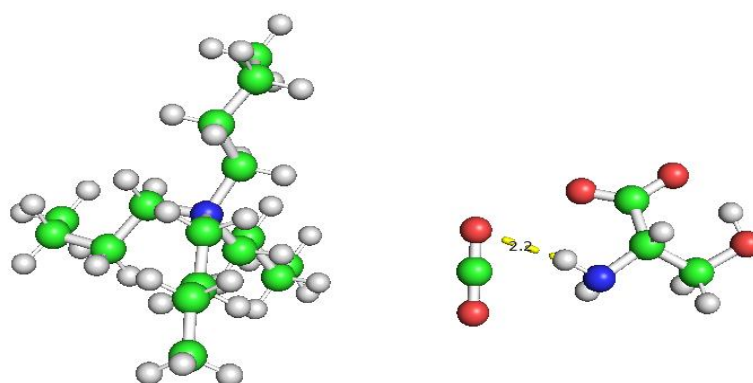
(D) [P₄₄₄₄] [GLY]-CO₂ (bond length in Å of anion-CO₂, 1.9)



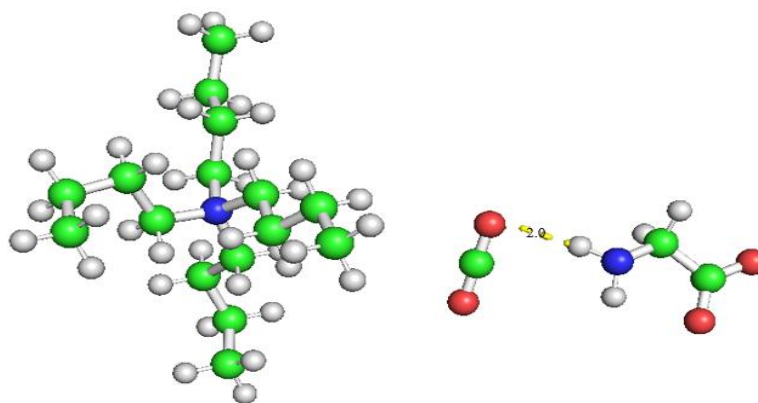
(E) [N₄₄₄₄] [ASP]-CO₂ (bond length in Å of anion-CO₂, 2.8)



(F) [N₄₄₄₄] [PHE]-CO₂ (bond length in Å of anion-CO₂, 2.4)



(G) [N₄₄₄₄] [SER]-CO₂ (bond length in Å of anion-CO₂, 2.2)



(H) [N₄₄₄₄] [GLY]-CO₂ (bond length in Å of 2.0)

Figure 23. Optimised structures of 8 AAIL (cation + anion + CO₂) complexes, which are (A) [P₄₄₄₄] [ASP]-CO₂, (B) [P₄₄₄₄] [PHE] -CO₂, (C) [P₄₄₄₄] [SER] -CO₂, (D) [P₄₄₄₄] [GLY] -CO₂, (E) [N₄₄₄₄] [ASP] -CO₂, (F) [N₄₄₄₄] [PHE] -CO₂, (G) [N₄₄₄₄] [SER] -CO₂, and (H) [N₄₄₄₄] [GLY] -CO₂.

* Bond between hydrogen attached to NH₂ group in anion with oxygen attached in CO₂ molecule.

Table 9. Henry constant and Gibbs free energy results.

AAILs	Henry constant (bar)	Gibbs free energy
[N ₄₄₄₄][PHE]	22.3	71.5
[N ₄₄₄₄][ASP]	22.0	66.8
[N ₄₄₄₄][SER]	21.7	66.3
[N ₄₄₄₄][GLY]	21.2	70.2
[P ₄₄₄₄][PHE]	21.6	70.3
[P ₄₄₄₄][ASP]	21.1	65.7
[P ₄₄₄₄][SER]	21.0	65.1
[P ₄₄₄₄][GLY]	20.5	69.0

*Henry constant- low value indicates higher CO₂ solubility.

*Gibbs free energy- low value indicates less stability of the AAILs.

Table 9 presents the Henry constant reflecting the solubility of CO₂ and the Gibbs free energy indicating the stability of the selected eight AAILs.

The solubility of gas in AAILs relies on their free volume and size, which impacts the physical absorption. Smaller ILs exhibit stronger CO₂ absorption due to their greater free volume. Hydrophilic ILs like serinate, glycinate, and aspartate, with small sizes and extra functional groups on the anions, show high CO₂ selectivity (CO₂/N₂) [46]. Henry's law constant (H) indicates physical absorption, while reaction equilibrium constant (K_x) signifies chemical absorption [47]. A high Henry constant value indicates that an AAIL favours chemisorption over physisorption in CO₂ capture [41,47].

In the results above, [GLY] exhibits the lowest Henry constant, indicating higher CO₂ solubility, while [PHE] shows the highest, suggesting lower CO₂ solubility. However, [PHE] contributes more to chemisorption due to the higher Henry constant value. This aligns with findings from a previous study [14], which noted that larger anions lead to increased viscosity, resulting in stronger interactions between the anion and the cation. Specifically, [PHE] has higher viscosity, while [GLY] has a lower viscosity, indicating higher ion mobility and CO₂ capture ability. Complex molecules with higher molecular weights and functional groups exhibit lower CO₂ capture ability due to increased electrostatic, hydrogen bonding, and van der Waals interactions, leading to lower ion mobility and free volume. Despite [P₄₄₄₄][PHE] exhibiting low CO₂ solubility, experimental results from a previous study showed that [P₄₄₄₄][

[ASP] has the highest viscosity (7437 mPa.s), followed by [P₄₄₄₄][PHE] (927 mPa.s), [P₄₄₄₄][SER] (902 mPa.s), and [P₄₄₄₄][GLY] (415 mPa.s), as presented in Table 7.

[P₄₄₄₄][ASP] exhibits the strongest cation-anion interaction (-1.016 kcal mol⁻¹) with a shorter bond length (5.7 Å), leading to reduced free volume, less stable, and able to capture less CO₂. Despite a higher Henry constant indicating lower CO₂ solubility, [P₄₄₄₄][ASP] highly contributes to physisorption due to the higher ILs-CO₂ interaction energy (-1.144 kcal mol⁻¹) and higher viscosity from hydrogen and electrostatic interactions.

In contrast, [P₄₄₄₄][PHE] shows a weaker cation-anion interaction (-0.006 kcal mol⁻¹) and longer bond length (6.0 Å), resulting in higher free volume and lower viscosity. Despite having the highest Henry constant among the ILs, [P₄₄₄₄][PHE] favours chemisorption due to the lowest ILs-CO₂ interaction energy (-0.061 kcal mol⁻¹). This aligns with prior findings indicating that longer alkyl chains enhance CO₂ solubility and higher Henry constants favour chemisorption [28, 41, 47]. Thus, [P₄₄₄₄][PHE] is the most stable among the four anions.

[P₄₄₄₄][SER] exhibits a lower cation-anion interaction energy (0.001 kcal mol⁻¹) and a longer bond length (6.2 Å) compared to [P₄₄₄₄][PHE]. With higher free volume and a strong ILs-CO₂ interaction (-1.193 kcal mol⁻¹), it favours physisorption and has the second lowest Henry constant value. This indicates good CO₂ capture ability due to the shorter alkyl chain and (OH) functional group, promoting hydrogen

bonding with cations, water, and CO₂. Consequently, [SER] is the least stable out of all the four anions. Conversely, [P₄₄₄₄][GLY] displays the lowest cation-anion interaction energy (0.072 kcal mol⁻¹) and the longest bond length (6.6 Å) among the AAILs. It exhibits higher CO₂ solubility (lowest Henry constant), is more favourable towards chemisorption, and lack of functional groups results in lower viscosity, higher ion mobility, and CO₂ capture [28,41,47]. This suggests that [P₄₄₄₄][GLY] is the second most stable AAIL. Reference [48] stated that the interaction between [GLY] and CO₂ forms strong intermolecular complexes, involving intramolecular proton transfer from the -NH₂ moiety of [GLY] to the carboxylate O atom. The longer side chain in [P₄₄₄₄] provides greater free volume, enhancing CO₂ absorption. However, water presence in ILs may reduce electrostatic interaction due to increased anion-water interaction, thereby decreasing interaction between the cation and anion.

[N₄₄₄₄] generally exhibits higher viscosity and lower ion mobility compared to [P₄₄₄₄]. This is due to nitrogen's higher electronegativity, which limits strong electrostatic interactions with anions and CO₂. On the other hand, [P₄₄₄₄] with phosphorus having lower electronegativity and higher polarisability shows more evenly distributed electron density, enhancing interactions with anions and CO₂. The explanation regarding bond length and cation-anion interaction is the same as mentioned before. The only difference here is [N₄₄₄₄] [SER] has the lowest ILs-CO₂ interaction (-0.075 kcal mol⁻¹) compared to other AAILs which may contribute to chemisorption due to the (OH) group attached in the anion chain and the higher electronegative which can lead to stronger chemical bonding interactions with the CO₂. This stronger chemical bonding can drive the reaction to chemisorption. But [N₄₄₄₄] [GLY] and [N₄₄₄₄] [PHE] have slightly higher ILs-CO₂ interaction of -0.132 kcal mol⁻¹ and -0.141 kcal mol⁻¹, respectively. Finally, [N₄₄₄₄] [ASP] has the highest ILs-CO₂ interaction (-1.132 kcal mol⁻¹), which is more favourable to physisorption.

CONCLUSION

The COSMO-RS approach can be utilised as an initial screening tool to identify the performance between an anion and a cation in the formation of new ILs. This study is anticipated to provide the first screening tool for systematically evaluating potential AAILs for direct capture of CO₂ by utilising the COSMO-RS computational study. The performance of AAILs in terms of absorption of CO₂ will be predicted from the COSMO-RS simulation. The study also covered the DFT and molecular modelling of AAILs. The significance of this study is that it should be capable of reducing time and expense in determining acceptable AAILs, particularly from many possibilities. It should also boost the chances of finding and exploring new TSILs. To summarise, 8 best performance AAILs (2 cations paired with 4 AA anions) in CO₂ capture

from COSMO-RS results were further analysed for their interaction energy in DFT calculations and bond length in molecular modelling using the Tmolex and Pymol softwares. The 8 AAILs were chosen based on 2 important parameters, which were PI and Henry constant, as the study mainly covered CO₂ capture. The AAILs are [P₄₄₄₄] paired with [ASP], [GLY], [PHE], and [SER] with Henry constant values of 21.1, 20.5, 21.6 and 21.0, and [N₄₄₄₄] paired with [ASP], [GLY], [PHE], and [SER] with Henry constant values of 22.0, 21.2, 22.3 and 21.7, respectively. The integration of COSMO-RS, DFT, and molecular modelling provides a comprehensive approach to identifying and analyse promising AAILs for CO₂ capture. By combining computational simulations and theoretical calculations, this study streamlines the selection process, saving time, and resources while increasing the potential for discovering novel TSILs with enhanced CO₂ capture capabilities.

ACKNOWLEDGEMENT

The authors would like to thank the Centre of Research in Ionic Liquids (CORIL) and the UTP Graduate Research Assistantship Scheme (015LC0-434) for supporting this study.

REFERENCES

1. Helmenstine, A. (2021) Chemical Composition of Air. *Science Notes and Projects, February 1, 2021*.
2. Saklani, N. & Khurana, A. (2019) Global Warming: Effect on Living Organisms, Causes and its Solutions. *International Journal of Engineering and Management Research, 09(05)*.
3. Xu, X., Myers, M. B., Versteeg, F., Adam, E., White, C., Crooke, E. & Colin David Wood (2021) Next generation amino acid technology for CO₂ capture. *Journal of Materials Chemistry. A, Materials for Energy and Sustainability, 9(3)*, 1692–1704.
4. Abu Sheha, M. A. & Tsokos, C. P. (2019) Statistical Modeling of Emission Factors of Fossil Fuels Contributing to Atmospheric Carbon Dioxide in Africa. *Atmospheric and Climate Sciences, 09(03)*, 438–455.
5. Jamaludin, S. N. & Mohd Salleh, R. (2016) Research Trends of Carbon Dioxide Capture using Ionic Liquids and Aqueous Amine-Ionic Liquids Mixtures. *Scientific Research Journal, 13(1)*, 53.
6. Recker, E. A., Green, M., Soltani, M., Paull, D. H., McManus, G. J., Davis, J. H. & Mirjafari, A. (2022) Direct Air Capture of CO₂ via Ionic Liquids Derived from “Waste” Amino Acids.

- ACS Sustainable Chemistry & Engineering*, **10(36)**, 11885–11890.
7. Qu, Y., Lan, J., Chen, Y. & Sun, J. (2021) Amino acid ionic liquids as efficient catalysts for CO₂ capture and chemical conversion with epoxides under metal/halogen/cocatalyst/solvent-free conditions. *Sustainable Energy & Fuels*, **5(9)**, 2494–2503.
 8. Zhang, R., Ke, Q., Zhang, Z., Zhou, B., Cui, G. & Lu, H. (2022) Tuning Functionalized Ionic Liquids for CO₂ Capture. *International Journal of Molecular Sciences*, **23(19)**, 11401–11401.
 9. Llaver, M., Fiorentini, E. F., Quintas, P. Y., Oviedo, M. N., Botella Arenas, M. B. & Wuilloud, R. G. (2022) Task-specific ionic liquids: Applications in sample preparation and the chemistry behind their selectivity. *Advances in Sample Preparation*, **1**, 100004.
 10. Hussain, M. A., Soujanya, Y. & Sastry, G. N. (2011) Evaluating the Efficacy of Amino Acids as CO₂ Capturing Agents: A First Principles Investigation. *Environmental Science & Technology*, **45(19)**, 8582–8588.
 11. Yang, Z. -Z., Zhao, Y. -N. & He, L. -N. (2011) CO₂ chemistry: task-specific ionic liquids for CO₂ capture/activation and subsequent conversion. *RSC Advances*, **1(4)**, 545.
 12. Kirchhecker, S. & Esposito, D. (2016) Amino acid based ionic liquids: A green and sustainable perspective. *Current Opinion in Green and Sustainable Chemistry*, **2**, 28–33.
 13. Khan, H. W., Reddy, A. V. B., Nasef, M. M. E., Bustam, M. A., Goto, M. & Moniruzzaman, M. (2020) Screening of ionic liquids for the extraction of biologically active compounds using emulsion liquid membrane: COSMO-RS prediction and experiments. *Journal of Molecular Liquids*, **309**, 113122.
 14. Salehin, F. N. M., Jumbri, K., Ramli, A., Daud, S. & Abdul Rahman, M. B. (2019) In silico solvation free energy and thermodynamics properties of H₂S in cholinium-based amino acid ionic liquids. *Journal of Molecular Liquids*, **294**, 111641.
 15. Muhammad Syahir Aminuddin, Man, Z., Mohamad & Abdullah, B. (2021) Screening of Metal Chloride Anion-based Ionic Liquids for Direct Conversion of Hydrogen Sulfide by COSMO-RS. *E3S Web of Conferences*, **287**, 02003–02003.
 16. Krishnan, S. (2019) A Comparison of Ultrasonic Mediated Lipid Extraction Efficiency from *Chlorella Vulgaris* Against Conventional Methods with Imidazolium Based Ionic Liquid as Additive. *Universiti Teknologi Petronas*.
 17. Islam, N., Warsi Khan, H., Gari, A. A., Yusuf, M. & Irshad, K. (2022) Screening of ionic liquids as sustainable greener solvents for the capture of greenhouse gases using COSMO-RS approach: Computational study. *Fuel*, **330**, 125540.
 18. Sumon, K. Z. & Henni, A. (2011) Ionic liquids for CO₂ capture using COSMO-RS: Effect of structure, properties and molecular interactions on solubility and selectivity. *Fluid Phase Equilibria*, **310(1-2)**, 39–55.
 19. Fasman, G. D., Practical Handbook of Biochemistry and Molecular Biology. *Cleveland: CRC Press*.
 20. Yang, Z. & Dai, S. (2021) Challenges in engineering the structure of ionic liquids towards direct air capture of CO₂. *Green Chemical Engineering*, **2(4)**, 342–345.
 21. Le Donne, A. & Bodo, E. (2021) Cholinium amino acid-based ionic liquids. *Biophysical Reviews*, **13(1)**, 147–160.
 22. Noorani, N. & Mehrdad, A. (2022) Cholinium-amino acid ionic liquids as biocompatible agents for carbon dioxide absorption. *Journal of Molecular Liquids*, **357**, 119078.
 23. Zhang, Y., Wu, Z., Chen, S., Yu, P. & Luo, Y. (2013) CO₂ Capture by Imidazolate-Based Ionic Liquids: Effect of Functionalized Cation and Dication. *Industrial & Engineering Chemistry Research*, **52(18)**, 6069–6075.
 24. Yunus, N. M., Mutalib, M. I. A., Man, Z., Bustam, M. A. & Murugesan, T. (2012) Solubility of CO₂ in pyridinium based ionic liquids. *Chemical Engineering Journal*, **189-190**, 94–100.
 25. Tomé, L. C., Mecerreyes, D., Carmen S. R. Freire, Paulo, L. & Marrucho, I. M. (2013) Pyrrolidinium-based polymeric ionic liquid materials: New perspectives for CO₂ separation membranes. *Journal of Membrane Science*, **428**, 260–266.
 26. Nasir M. Tukur, Saidu M. Waziri & Esam Z. Hamad (2005) Predicting Solubilities in Polymer Systems Using COSMO-RS [Review of Predicting Solubilities in Polymer Systems Using COSMO-RS]. *AICHE*.
 27. Mohan, M. D., Keasling, J. A., Simmons, B. & Singh, S. (2022) In silico COSMO-RS predictive screening of ionic liquids for the dissolution of plastic. *Green Chemistry*, **24(10)**, 4140–4152.
 28. Zhang, X., Liu, Z. & Wang, W. (2008) Screening of ionic liquids to capture CO₂ by COSMO-

- RS and experiments. *AIChE Journal*, **54**(10), 2717–2728.
29. Salehin, F. N. B. M. (2020) An Insight into Solubility and Selectivity of H₂S/CO₂ in Cholinium-based Amino Acid Ionic Liquids from Molecular Dynamics Simulation. *Universiti Teknologi Petronas*.
30. Mohamed Hatta, N. S., Aroua, M. K., Hussin, F. & Gew, L. T. (2022) A Systematic Review of Amino Acid-Based Adsorbents for CO₂ Capture. *Energies*, **15**(10), 3753.
31. Liu, Z., Teng, Y., Zhang, K., Cao, Y. & Pan, W. (2013) CO₂ adsorption properties and thermal stability of different amine-impregnated MCM-41 materials. *Journal of Fuel Chemistry and Technology*, **41**(4), 469–475.
32. Ventura, M., Marques, C. S., Rosatella, A. A., Carlos, Gonçalves, F. & Coutinho, P. (2012) Toxicity assessment of various ionic liquid families towards *Vibrio fischeri* marine bacteria. *Ecotoxicology and Environmental Safety*, **76**, 162–168.
33. Stefano Onofri & Bodo, E. (2021) CO₂ Capture in Biocompatible Amino Acid Ionic Liquids: Exploring the Reaction Mechanisms for Bimolecular Absorption Processes. *The Journal of Physical Chemistry B*, **125**(21), 5611–5619.
34. Yoon, B. & Voth, G. A. (2023) Elucidating the Molecular Mechanism of CO₂ Capture by Amino Acid Ionic Liquids. *Journal of the American Chemical Society*, **145**(29), 15663–15667.
35. Zhang, Y., Zhang, S., Lu, X., Zhou, Q., Fan, W. & Zhang, X. (2009) Dual Amino-Functionalised Phosphonium Ionic Liquids for CO₂ Capture. *Chemistry - a European Journal*, **15**(12), 3003–3011.
36. Rahman, M. B. A., Jumbri, K., Basri, M., Abdulmalek, E., Sirat, K. & Salleh, A. B. (2010) Synthesis and Physico-Chemical Properties of New Tetraethylammonium-Based Amino Acid Chiral Ionic Liquids. *Molecules*, **15**(4), 2388–2397.
37. Ohno, H. & Fukumoto, K. (2007) Amino Acid Ionic Liquids. *Accounts of Chemical Research*, **40**(11), 1122–1129.
38. Zhang, J., Zhang, S., Dong, K., Zhang, Y., Shen, Y. & Lv, X. (2006) Supported Absorption of CO₂ by Tetrabutylphosphonium Amino Acid Ionic Liquids. *Chemistry - a European Journal*, **12**(15), 4021–4026.
39. Kagimoto, J., Fukumoto, K. & Ohno, H. (2006) Effect of tetrabutylphosphonium cation on the physico-chemical properties of amino-acid ionic liquids. *Chemical Communications*, **21**, 2254.
40. Fu, Y., Yang, Z., Mahurin, S. M., Dai, S. & Jiang, D. (2022) Ionic liquids for carbon capture. *MRS Bulletin*, **47**(4).
41. Noorani, N. & Mehrdad, A. (2020) CO₂ solubility in some amino acid-based ionic liquids: Measurement, correlation and DFT studies. *Fluid Phase Equilibria*, **517**, 112591.
42. An, X., Wang, P., Ma, X., Du, X., Hao, X., Yang, Z. & Guan, G. (2023) Application of ionic liquids in CO₂ capture and electrochemical reduction: A review. *Carbon Resources Conversion*, **6**(2), 85–97.
43. Heba Al-Fnaish & Lue, L. (2017) Modelling the solubility of H₂S and CO₂ in ionic liquids using PC-SAFT equation of state. *Fluid Phase Equilibria*, **450**, 30–41.
44. Hunt, P. A., Ashworth, C. R. & Matthews, R. P. (2015) Hydrogen bonding in ionic liquids. *Chemical Society Reviews*, **44**(5), 1257–1288.
45. Steiner, T. (2002) The Hydrogen Bond in the Solid State. *Angewandte Chemie International Edition*, **41**(1), 48–76.
46. Abdul Rajjak Shaikh, Eiji Kamio, Hiromitsu Takaba & Matsuyama, H. (2015) Effects of Water Concentration on the Free Volume of Amino Acid Ionic Liquids Investigated by Molecular Dynamics Simulations. *The Journal of Physical Chemistry B*, **119**(1), 263–273.
47. Noorani, N., Mehrdad, A. & Ahadzadeh, I. (2021) CO₂ absorption in amino acid-based ionic liquids: Experimental and theoretical studies. *Fluid Phase Equilibria*, **547**, 113185.
48. Abdul Rajjak Shaikh, Ashraf, M., Turki AlMayef, Chawla, M., Poater, A. & Cavallo, L. (2020) Amino acid ionic liquids as potential candidates for CO₂ capture: Combined density functional theory and molecular dynamics simulations. *Chemical Physics Letters*, **745**, 137239–137239.